Atmospheric
Chemistry
and Physics

Investigation of the *β*-pinene photooxidation by OH in the atmosphere simulation chamber SAPHIR

Martin Kaminski[1,a], **Hendrik Fuchs**[1], **Ismail-Hakki Acir**[1,b], **Birger Bohn**[1], **Theo Brauers**[1,†], **Hans-Peter Dorn**[1], **Rolf Häseler**[1], **Andreas Hofzumahaus**[1], **Xin Li**[1,c], **Anna Lutz**[2], **Sascha Nehr**[1,d], **Franz Rohrer**[1], **Ralf Tillmann**[1], **Luc Vereecken**[1], **Robert Wegener**[1], and **Andreas Wahner**[1]

[1]Institute of Energy and Climate Research, IEK-8: Troposphere, Forschungszentrum Jülich GmbH, Jülich, Germany
[2]Department of Chemistry and Molecular Biology, University of Gothenburg, Gothenburg, Sweden
[a]now at: Bundesamt für Verbraucherschutz, Abteilung 5 – Methodenstandardisierung,
Referenzlaboratorien und Antibiotikaresistenz, Berlin, Germany
[b]now at: Institute of Nutrition and Food Sciences, Food Chemistry, University of Bonn, Bonn, Germany
[c]now at: State Key Joint Laboratory of Environmental Simulation and Pollution Control, College of Environmental Sciences
and Engineering, Peking University, Beijing, China
[d]now at: Verein Deutscher Ingenieure e.V., Kommission Reinhaltung der Luft, Düsseldorf, Germany
[†]deceased

Correspondence to: Robert Wegener (r.wegener@fz-juelich.de)

Abstract. Besides isoprene, monoterpenes are the non-methane volatile organic compounds (VOCs) with the highest global emission rates. Due to their high reactivity towards OH, monoterpenes can dominate the radical chemistry of the atmosphere in forested areas. In the present study the photochemical degradation mechanism of *β*-pinene was investigated in the Jülich atmosphere simulation chamber SAPHIR (Simulation of Atmospheric PHotochemistry In a large Reaction Chamber). One focus of this study is on the OH budget in the degradation process. Therefore, the SAPHIR chamber was equipped with instrumentation to measure radicals (OH, HO_2, RO_2), the total OH reactivity, important OH precursors (O_3, $HONO$, $HCHO$), the parent VOC *β*-pinene, its main oxidation products, acetone and nopinone and photolysis frequencies. All experiments were carried out under low-NO conditions (≤ 300 ppt) and at atmospheric *β*-pinene concentrations (≤ 5 ppb) with and without addition of ozone. For the investigation of the OH budget, the OH production and destruction rates were calculated from measured quantities. Within the limits of accuracy of the instruments, the OH budget was balanced in all *β*-pinene oxidation experiments. However, even though the OH budget was closed, simulation results from the Master Chemical Mechanism (MCM) 3.2 showed that the OH production and destruction rates were underestimated by the model. The measured OH and HO_2 concentrations were underestimated by up to a factor of 2, whereas the total OH reactivity was slightly overestimated because the model predicted a nopinone mixing ratio which was 3 times higher than measured. A new, theory-derived, first-generation product distribution by Vereecken and Peeters (2012) was able to reproduce the measured nopinone time series and the total OH reactivity. Nevertheless, the measured OH and HO_2 concentrations remained underestimated by the numerical simulations. These observations together with the fact that the measured OH budget was closed suggest the existence of unaccounted sources of HO_2. Although the mechanism of additional HO_2 formation could not be resolved, our model studies suggest that an activated alkoxy radical intermediate proposed in the model of Vereecken and Peeters (2012) generates HO_2 in a new pathway, whose importance has been underestimated so far. The proposed reaction path involves unimolecular rearrangement and decomposition reactions and photolysis of dicarbonyl products, yielding additional HO_2 and CO. Further experiments and quantum chemical calculations have to be made to completely unravel the pathway of HO_2 formation.

1   Introduction

Thousands of different volatile organic compounds (VOCs) are emitted into the atmosphere (Goldstein and Galbally, 2007). The emissions of biogenic volatile organic compounds (BVOCs) exceed those of anthropogenic VOCs by a factor of 10 (Piccot et al., 1992; Guenther et al., 1995, 2012). On a global scale, isoprene and monoterpenes are the BVOCs with the highest emission rates, with the exception of methane. About 44 % of the global BVOC emissions can be attributed to isoprene and about 11 % to monoterpenes (Guenther et al., 1995). Isoprene and monoterpenes are unsaturated hydrocarbons. Hence, their main atmospheric sink is the addition of hydroxyl radicals (OH), nitrate radicals (NO_3) or ozone to the double bond (Calogirou et al., 1999; Atkinson and Arey, 2003). During daytime the reaction of isoprene and monoterpenes with the OH radical is the major sink for these VOC species. The subsequent addition of oxygen produces organic peroxy radicals (RO_2). In the presence of nitrogen oxides (NO_x), RO_2 is indirectly converted to hydroperoxy radicals (HO_2) through reaction with NO. HO_2 reacts further with NO, recycling the OH consumed in the initial reaction step and producing further NO_2. As a side effect, ozone is produced by NO_2 photolysis. The oxidation of VOCs in the presence of NO is the main photochemical source of ozone in the troposphere (Seinfeld and Pandis, 2006). Moreover, the oxidation processes of isoprene and monoterpenes mainly lead to the production of less reactive polar oxygenated volatile organic compounds (OVOCs), which are significantly involved in the formation of secondary organic aerosols (SOA) (Kanakidou et al., 2005; Goldstein and Galbally, 2007).

During the last decade, the research on the chemical degradation of BVOCs in the atmosphere has seen significant progress through laboratory and atmospheric chamber experiments as well as theoretical chemistry studies. It was discovered that RO_2 radicals from the reaction of BVOCs with OH can undergo unimolecular reactions which influence the chemistry of HO_x and OVOCs. In the case of the degradation of isoprene and methacrolein, RO_2 was found to efficiently regenerate HO_x by isomerization and decomposition reactions (Paulot et al., 2009; da Silva et al., 2010; Peeters and Müller, 2010; Crounse et al., 2011, 2012, 2013; Wolfe et al., 2012; Taraborrelli et al., 2012; Liu et al., 2013; Fuchs et al., 2013, 2014; Peeters et al., 2014). RO_2 radicals from the oxidation of isoprene and some monoterpenes were found to produce low-volatility OVOCs, which contribute substantially to SOA formation in the atmosphere (Paulot et al., 2009; Ehn et al., 2014; Bates et al., 2014). The discovered chemistry is particularly important in forests, which contribute to the global non-methane BVOC emissions with an estimated share of 75 % (Guenther et al., 1995; Wiedinmyer et al., 2004; Guenther et al., 2012). In forests, the unimolecular RO_2 reactions can effectively compete with the

$RO_2 +$ NO reaction, since anthropogenic NO emissions are generally missing.

The above-mentioned studies of BVOC oxidation mechanisms were mostly inspired by field observations of unexplained high OH concentrations in isoprene-dominated forests, which have pointed to unknown NO-independent OH recycling processes (Tan et al., 2001; Carslaw et al., 2001; Ren et al., 2008; Lelieveld et al., 2008; Hofzumahaus et al., 2009; Kubistin et al., 2010; Whalley et al., 2011; Lu et al., 2012). The newly discovered mechanisms for isoprene and methacrolein, however, can explain only part of the observed high OH concentrations. Another possible reason could be OH interferences in the low-pressure laser-induced fluorescence (LIF) instruments that were applied in the above field studies. Artificial OH production was discovered in two similar LIF instruments applying a newly developed chemical modulation technique for OH detection (Mao et al., 2012; Hens et al., 2014; Novelli et al., 2014; Feiner et al., 2016). The interference seems to be related to organic compounds, but the underlying OH formation mechanism is not known. Experimental tests with other types of LIF instruments have not found such interference (Fuchs et al., 2012, 2016; Griffith et al., 2013; Tan et al., 2017), yet it is difficult to draw firm conclusions from past campaigns as long as the reported artifacts (Mao et al., 2012) are not fully understood.

Due to their abundance and their structural similarity to isoprene, unknown monoterpene chemistry may contribute to the underestimation of OH concentrations in forests as proposed by da Silva et al. (2010) for open-chain monoterpenes like myrcene and ocimene. During a field campaign in Borneo, Whalley et al. (2011) observed that discrepancies between measured and modeled OH occurred in the morning hours when VOC emissions were dominated by monoterpenes. Moreover, field studies in Greece (Carslaw et al., 2001), in the US (Kim et al., 2013) and in Finland (Hens et al., 2014) indicate that the radical chemistry in forested areas, which are dominated by monoterpene and 2-methyl-3-buten-2-ol (MBO) emissions, is not well understood.

In this work we investigated the atmospheric degradation of monoterpenes in the atmosphere simulation chamber SAPHIR (Simulation of Atmospheric PHotochemistry In a large Reaction Chamber) in Jülich. β-Pinene comprises 17 % of the estimated global monoterpene emission rate (Sindelarova et al., 2014) and was therefore chosen as a representative species for our investigations. To our knowledge it is the first chamber study investigating β-pinene, or any monoterpene degradation in general, under natural concentration conditions (VOC less than 5 ppb). In comparison to other chamber studies which focused on the determination of products and SOA yields (Lee et al., 2006; Saathoff et al., 2009; Eddingsaas et al., 2012a, b; Zhao et al., 2015), our main goal was to investigate the radical budget of the monoterpene degradation. For that purpose all critical radical species (OH, HO_2, RO_2) were measured. In order to exclude possible measurement artifacts for OH, differential optical absorption

spectroscopy (DOAS) was applied for OH measurements in addition to LIF.
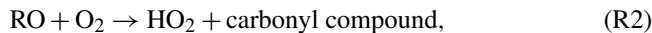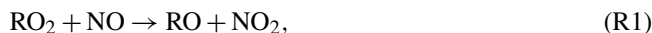
2 Methods

2.1 SAPHIR atmosphere simulation chamber

The Simulation of Atmospheric PHotochemistry In a large Reaction chamber located in the Forschungszentrum Jülich (Germany) is a tool to investigate complex atmospheric mechanisms under nearly natural conditions. The chamber has a cylindric shape (18 m length, 5 m diameter, 270 m^3 volume) and consists of a double-walled FEP (fluorinated ethylene propylene) Teflon foil attached to a steel frame. The Teflon foil guarantees a maximum inertness of the chamber surface and leads to a minimization of wall effects. In SAPHIR natural sunlight is used as a light source for photochemical reactions. About 85 % of the UV-A, UV-B and visible light is transmitted by the FEP foil. A shutter system allows us to switch between illuminated and dark chamber conditions within 60 s. To investigate photochemical degradation processes in the ppb and sub-ppb range, SAPHIR is operated with ultra-pure synthetic air (Linde, N$_2$ 99.9999 %, O$_2$ 99.9999 %). A slight overpressure of about 30 Pa in the inner chamber prevents diffusion of outside air into SAPHIR. Due to small leakages and consumption of air by instruments, a replenishment flow has to be introduced into the chamber to keep up the pressure difference to the outside. During experimental operation this flow is in a range of 9–12 m^3 h^{-1}, leading to a dilution of trace gases at a rate of approximately 3–4 % h^{-1}. An installed ventilator guarantees well-mixed conditions during the experiments. For more detailed information about the chamber and its properties, the reader is referred to previous publications (Poppe et al., 2007; Schlosser et al., 2007, 2009; Wegener et al., 2007; Dorn et al., 2013).

2.2 Instrumentation

OH, HO$_2$ and RO$_2$ concentrations were measured simultaneously by a laser-induced fluorescence system, using three independent low-pressure detection cells. Each cell samples ambient air by gas expansion through an inlet nozzle, producing a fast gas flow through the cell. OH is detected by pulsed laser-excited resonance fluorescence at 308 nm (Holland et al., 1995). RO$_2$ and HO$_2$ are detected indirectly by chemical conversion with NO to OH, followed by LIF detection of the formed OH (Fuchs et al., 2008, 2011). The peroxy radicals are distinguished from each other by their different conversion efficiencies, which depend on the amount of added NO and the reaction time between NO addition and OH detection. In the low-pressure HO$_x$ cell, the addition of NO leads to fast formation of OH in just one reaction step. In contrast, conversion of RO$_2$ to OH requires at least three reaction steps:

$$RO_2 + NO \rightarrow RO + NO_2, \tag{R1}$$

$$RO + O_2 \rightarrow HO_2 + \text{carbonyl compound}, \tag{R2}$$

$$HO_2 + NO \rightarrow OH + NO_2. \tag{R3}$$

For simple alkyl peroxy radicals, this reaction sequence is relatively slow (especially at reduced O$_2$ partial pressure) compared to the residence time in the HO$_2$ detection cell and results in a very low detection efficiency. However, β-hydroxy RO$_2$ species produced by the reaction of alkenes with OH are converted by NO to highly reactive β-hydroxy alkoxy radicals. Instead of reacting with O$_2$ directly, β-hydroxy alkoxy radicals nearly exclusively decompose and then react rapidly with O$_2$, thereby forming HO$_2$ much faster than other alkoxy radicals. The fact that for β-hydroxy alkyl peroxy radicals the overall conversion to OH is very fast leads to an interference in the HO$_2$ channel of the LIF instrument (Fuchs et al., 2011). The interference was carefully characterized for RO$_2$ species formed by the reaction of β-pinene with OH in laboratory experiments following the procedure described by Fuchs et al. (2011). About 25 % of these RO$_2$ species are detected as an additional signal in the HO$_2$ channel of the instrument. In the third measurement cell, the sum of atmospheric RO$_2$ and HO$_2$ is measured. In this case, RO$_2$ radicals are converted by NO in a pre-reactor to HO$_2$, which is then further converted together with atmospheric HO$_2$ to OH in the detection cell (Fuchs et al., 2008). Since the RO$_2$ concentration is calculated as the difference between the concentration of RO$_x$ (RO$_2$ + HO$_2$) and measured HO$_2$, the interference in the HO$_2$ measurement also affects the RO$_2$ data indirectly.

On 27 August 2012 OH was measured additionally by a differential optical absorption spectrometer. In general both instruments showed a good agreement over the past 10 years (Schlosser et al., 2007, 2009; Fuchs et al., 2012). Additionally, for the terpenoid campaign in 2012, on average no significant difference between the LIF and DOAS instrument was observed. As the DOAS instrument is the only absolute method for the quantification of OH (Hofzumahaus and Heard, 2016), the DOAS OH data were used for the following evaluation of the OH budget analysis.

The OH reactivity k(OH) was measured by the flash photolysis/laser-induced fluorescence technique (Lou et al., 2010). The evaluation of the pseudo-first-order decays of OH gives a direct measure of the total rate coefficient of the OH loss.

Besides OH, HO$_2$, RO$_2$ and k(OH), HCHO (Hantzsch reaction), HONO (long-path absorption photometry, LOPAP), CO (reduction gas analysis, RGA), CO$_2$, CH$_4$, and H$_2$O (cavity ring-down spectroscopy), as well as NO, NO$_2$ and O$_3$ (chemiluminescence) were determined by direct measurements. VOCs were measured by a PTR-TOF-MS (proton transfer reaction time-of-flight mass spectrome-

Table 1. Instrumentation for radical and trace-gas detection during the β-pinene oxidation experiments.

	Technique	Time resolution	1σ precision	1σ accuracy
OH	DOAS[a] (Dorn et al., 1995; Hausmann et al., 1997; Schlosser et al., 2007)	205 s	0.8×10^6 cm^{-3}	6.5 %
OH	LIF[b] (Lu et al., 2012)	47 s	0.3×10^6 cm^{-3}	13 %
HO$_2$, RO$_2$	LIF[b] (Fuchs et al., 2011, 2008)	47 s	1.5×10^7 cm^{-3}	16 %
k(OH)	Laser-photolysis + LIF[b] (Lou et al., 2010)	180 s	0.3 s^{-1}	0.5 s^{-1}
NO	Chemiluminescence (Rohrer and Brüning, 1992)	180 s	4 pptv	5 %
NO$_2$	Chemiluminescence (Rohrer and Brüning, 1992)	180 s	2 pptv	5 %
O$_3$	Chemiluminescence (Ridley et al., 1992)	180 s	60 pptv	5 %
VOCs	PTR-TOF-MS[c] (Lindinger et al., 1998; Jordan et al., 2009)	30 s	15 pptv	14 %
	GC[d] (Kaminski, 2014)	30 min	4–8 %	5 %
CO	RGA[e] (Wegener et al., 2007)	3 min	4 %	10 %
HONO	LOPAP[f] (Häseler et al., 2009)	300 s	1.3 pptv	10 %
HCHO	BB-DOAS[g] (Brauers et al., 2007)	100 s	20 %	6 %
Photolysis frequencies	Spectroradiometer (Bohn and Zilken, 2005)	60 s	10 %	10 %

[a] Differential optical absorption spectroscopy. [b] Laser-induced fluorescence. [c] Proton transfer reaction time-of-flight mass spectrometry. [d] Gas chromatography. [e] Reactive gas analyzer. [f] Long-path absorption photometer. [g] Broadband differential optical absorption spectroscopy.

try) and two gas chromatographs of the same type coupled with mass spectrometric and flame ionization detectors (GC/MS/FID). Moreover, experimental boundary conditions including temperature (ultrasonic anemometer), pressure (capacitive gauge), replenishment flow rate (mass flow controller) and photolysis frequencies (spectroradiometer) were continuously recorded.

Table 1 provides an overview of the key instruments for this study and their specifications. For more detailed information on the analytical instrumentation of SAPHIR, the reader is referred to previous publications (Bohn and Zilken, 2005; Bohn et al., 2005; Rohrer et al., 2005; Wegener et al., 2007; Dorn et al., 2013, and references therein).

2.3 Experimental procedure

Before every experiment day the chamber was flushed with dry ultra-pure synthetic air overnight to purge contaminants of previous experiments under their detection limit. At the beginning of the experiment 20 ppm of CO$_2$ was injected into SAPHIR as a dilution tracer. After that, the relative humidity was increased to 75 % by adding water vapor, gener-ated by the vaporization of ultra-pure water (Milli-Q), to the purge flow. As HONO photolysis is the main source of OH in the SAPHIR chamber it is impossible to conduct experiments in the complete absence of NO. To lower the NO level in the experiment on 27 August 50 ppb of ozone, produced from a silent discharge ozonizer (O3Onia), was injected after humidification. Shortly afterward the shutter system of SAPHIR was opened, exposing the chamber to sunlight.

In the following 2 h of the experiments (so-called "zero-air phase") no other trace gases were introduced into SAPHIR. During the zero-air period HONO was formed from the chamber walls (Rohrer et al., 2005), depending on relative humidity and UV radiation. In addition to the OH production the photolysis of HONO leads to an increase in NO and NO$_2$ concentration. In addition to HONO production, acetaldehyde, formaldehyde and acetone were also formed in the chamber with a rate of 90–250 ppt h^{-1}. The zero-air phase ended with the injection of β-pinene while the SAPHIR chamber was exposed to light. The injection was performed by introducing a high-concentration gas mixture of β-pinene (about 50 ppm) from a Silcosteel Canister (Restek) through a

mass flow controller to the experimental flow. The β-pinene concentration of the mixture was previously determined by oxidizing a part of the β-pinene mixture on a platinum catalyst and quantifying the produced CO_2. This absolute method makes it possible to calculate the VOC starting concentration of the experiment very accurately. During the following 6 h of the experiment, the so-called "VOC phase", β-pinene was degraded by OH in the illuminated chamber. In the experiment of 27 August β-pinene was injected for a second and third time into SAPHIR approximately 2 and 4 h after the first VOC injection, respectively. Every experiment ended with the closing of the louver system of the chamber in the late evening of the experiment day. For all the chamber experiments the fan was running during the whole time, ensuring homogeneous mixing of the chamber air.

Table 2 sums up the experimental conditions of the three β-pinene oxidation experiments.

2.4 Model calculations

The acquired time series of trace gases and radicals were compared to zero-dimensional box model simulations with the Master Chemical Mechanism (MCM). The MCM is a state-of-the-art chemical mechanism developed by Jenkin et al. (1997) and Saunders et al. (2003). For this publication the MCM version 3.2 (MCM 3.2) was used (available at http://mcm.leeds.ac.uk/MCMv3.2/). For the application on modeling chamber experiments the model was extended by some chamber-specific processes. As an alternative to the β-pinene chemistry in the MCM, we also applied the reaction mechanism by Vereecken and Peeters (2012), which is based on theoretical kinetic analyses of the reaction mechanism. The mechanism by Vereecken and Peeters (2012) only describes the first-generation product formation – i.e., the subsequent chemistry of the products formed in the first radical chain is not included in the model. The accumulated yield of primary products in our model runs remains below 20 % compared to the sum of the residual concentration of β-pinene and the concentrations of reactive primary products whose chemistry is fully described (e.g., nopinone and acetone). As such, it appears that omitting the secondary chemistry of these products does not have an overly large impact on the reaction fluxes and is therefore unlikely to be the main reason for any discrepancies relative to the measurements.

As mentioned in Sect. 2.1 the required replenishment flow into SAPHIR leads to an additional dilution process for every model species. The applied dilution rate is thereby calculated from the measured CO_2 loss in the chamber. Previous characterization experiments showed that ozone had a shorter lifetime than CO_2 in the chamber (dilution-corrected ozone lifetime of approximately 30 h). This observation was included as an additional loss term in the model. The chamber sources of HONO, HCHO and acetone are well known from routine reference experiments in SAPHIR and can be parameterized by empirical equations, depending on tem-

perature, relative humidity and solar radiation in the chamber (Rohrer et al., 2005; Karl et al., 2006; Kaminski, 2014). The source strengths were adjusted to match the time series of NO_x, HCHO and acetone during the zero-air phases of the experiments. The parameterization of the acetaldehyde source was less satisfactory, so the model was constrained by the measured acetaldehyde concentration.

In all experiments the summed contributions of known chamber sources to the OH reactivity measured in the zero-air phase (0.1–$0.7\,\mathrm{s}^{-1}$) were not sufficient to explain the measured OH reactivity (0.7–$1.5\,\mathrm{s}^{-1}$). Analogous to the procedure applied by Fuchs et al. (2012, 2014), the unexplained part of the measured OH reactivity was modeled as a co-reactant, Y, with constant OH reactivity in the model, where the concentration times rate coefficient, $[Y] \cdot k_{OH+Y}$, was set to reproduce the measured OH reactivity in the chamber after humidification. Analogous to CO, the reaction of Y with OH is assumed to form one molecule of HO_2.

The parameters temperature; pressure; water vapor concentration; the calculated dilution rate; and the photolysis frequencies for HONO, HCHO, O_3 and NO_2 were set as fixed boundary conditions in the model. Photolysis frequencies that were not measured were calculated for clear sky conditions by the function included in MCM version 3.1 and then corrected for cloud cover and the transmission of the Teflon film by multiplying the clear sky value by the ratio of measured to modeled photolysis frequency of NO_2. Constrained parameters were re-initialized on a 1 min time grid. The injections of β-pinene and ozone in the chamber were modeled as sources which were only present during the time period of injection. The source strengths were adapted to match the measured ozone concentration and the OH reactivity at the point of injection. The subsequent time series of the concentrations were determined by the kinetic models described above.

Because of described instrumental interferences it is not possible to directly compare the modeled HO_2 concentration, $[HO_2]$, and the sum of the concentrations of the different RO_2 species, $[RO_2]$, against the measured time series of the LIF instrument, $[HO_2^*]$ and $[RO_2^*]$, for HO_2 and RO_2, respectively.

$$[HO_2^*] = [HO_2] + \sum \left(\alpha_{RO_2}^i \cdot [RO_2]_i \right), \tag{1}$$

$$[RO_2^*] = [RO_2] - \sum \left(\alpha_{RO_2}^i \cdot [RO_2]_i \right), \tag{2}$$

where $\alpha_{RO_2}^i$ is the relative detection sensitivity for RO_2 species i (compared to HO_2 with $\alpha = 1$), $\sum [RO_2]_i$ are the interfering RO_2 radicals of β-pinene, and $\sum \left(\alpha_{RO_2}^i \cdot [RO_2]_i \right)$ is the RO_2 interference. For a direct comparison of the measured $[HO_2^*]$ against the model, the modeled HO_2 plus an estimated RO_2 interference is combined to yield the model parameter HO_2^* (Lu et al., 2012). Depending on the experimental phase, up to 25 % of the modeled HO_2^* can be attributed to the interfering RO_2 species, $[RO_{2i}]$. Moreover, note that

Table 2. Experimental conditions of the β-pinene oxidation experiments. Maximum values are given for β-pinene and averaged values for the part of the experiment, when β-pinene was present, for the other parameters.

β-pinene ppbv	OH $10^6\,\mathrm{cm}^{-3}$	NO_x ppbv	NO pptv	O_3 ppbv	RH %	$j(NO_2)$ $10^{-3}\,\mathrm{s}^{-1}$	T K	Date
4.3	6.0	1.0	300	10	45	5	295	12 Aug 2012
4.3	4.5	0.9	200	10	45	4	299	15 Aug 2012
4.7	3.5	0.9	100	40	40	4.5	293	27 Aug 2012

the MCM and the modifications by Vereecken and Peeters yield different RO_2 species, which results in rather different contributions of RO_2 into the HO_2 signal.

RO_2 radicals are detected in the LIF instrument by a three-step conversion of RO_2 to OH. Only species reacting with NO to RO and then decomposing or reacting with O_2 in a second reaction step to HO_2 can be detected with a sufficient sensitivity. Depending on the model used, up to 70 % of the modeled RO_2 species of β-pinene are not detectable under these conditions. To account for this, the measured RO_2 signal $[RO_2^*]$ is compared to the model parameter RO_2^*, which corresponds to the sum of the theoretically detectable RO_2 model species.

The model RO_2^* must be additionally corrected by the subtraction of the RO_2 species which are already included in the model parameter HO_2^*. This is again related to the operating conditions of the LIF instrument, where in the RO_x cell the sum of detectable RO_2 plus HO_2 and in the HO_x cell the HO_2 plus interfering RO_2 radicals are measured. As the RO_2 concentration is determined by subtracting the signal of the HO_x cell from the signal of the RO_x cell, an RO_2 interference in the HO_x cell automatically leads to an underestimation of the calculated RO_2 concentration.

3 Results and discussion

3.1 Determination of product yields

The formation yields of first-generation degradation products are important information for the understanding of the oxidation mechanism of β-pinene with OH (Fig. 1). By correlating the concentration of the products with the concentration of the degraded β-pinene, it is possible to determine the product yield. Because of the lack of suitable reference standards and the low concentration of β-pinene, it was only possible to determine the yield of acetone and nopinone in the OH oxidation experiment. The concentrations of β-pinene and nopinone were determined by PTR-TOF-MS, whereas interpolated GC/MS/FID data of the acetone concentration were used for the yield determination. This was done to exclude any possible interferences on the quantifier ion of acetone in the PTR-TOF-MS.

As a result of ozone addition in the experiment on 27 August 2012, a part of the injected β-pinene was degraded by ozonolysis. The fraction of the ozonolysis in the total conversion of β-pinene was approximately 5 % and can be neglected.

The experiment duration of several hours necessitated the correction of the measured concentration time series to account for reactive losses of acetone and nopinone with OH and chamber effects like dilution (all species) and chamber sources (acetone). This was done using a recursive discrete time equation analogous to Galloway et al. (2011). The correction of the acetone concentration was done by scaling the assumed acetone chamber source to the measured values during the zero-air phase of the experiments. The assumed acetone source strength was typically $70\,\mathrm{ppt\,h}^{-1}$, which was as large as 20 to 30 % of the total amount of acetone produced in the β-pinene experiments. Equations (3)–(7) illustrate all applied corrections on the acetone concentration.

$$[CH_3COCH_3]_{\mathrm{corr}(i)} = [CH_3COCH_3]_{\mathrm{corr}(i-1)} + \Delta c_{CH_3COCH_3}$$
$$+ \Delta c_{\mathrm{RL}} + \Delta c_{\mathrm{DIL}} + \Delta c_{S_{CH_3COCH_3}} \tag{3}$$

$$\Delta c_{\mathrm{RL}} = [CH_3COCH_3]_{(i-1)} \cdot [OH]_{(i-1)} \cdot \Delta t$$
$$\cdot k_{CH_3COCH_3+OH} \tag{4}$$

$$\Delta c_{\mathrm{DIL}} = [CH_3COCH_3]_{(i-1)} \cdot \Delta t \cdot k_{\mathrm{DIL}} \tag{5}$$

$$\Delta c_{S_{CH_3COCH_3}} = S_{CH_3COCH_3} \cdot \Delta t \tag{6}$$

$$S_{CH_3COCH_3} = a_{CH_3COCH_3} \cdot J_{NO_2} \cdot (0.21 + 2.6 \times 10^{-2} \cdot RH)$$
$$\cdot e^{(-2876/T)} \tag{7}$$

$[CH_3COCH_3]_{\mathrm{corr}}$ is the corrected acetone concentration, Δc_{RL} is the reactive loss, Δc_{DIL} is the dilution, $\Delta c_{S_{CH_3COCH_3}}$ is the chamber source, Δt is the time interval between time i and $(i-1)$, $S_{CH_3COCH_3}$ is the source strength, $a_{CH_3COCH_3}$ is the scaling factor, RH is the relative humidity, and J_{NO_2} is the photolysis frequency NO_2.

The results of the yield determination are listed in Table 3. In principle, product yields of nonlinear degradation processes depend on the fate of RO_2, which is governed by multiple physical and chemical boundary conditions such as pressure, temperature, H_2O, O_3, VOCs, HO_2 and NO concentration. The discussed β-pinene experiment was conducted at ambient pressure in a temperature range of 298–304 K. The relative humidity was about 50 % before the first VOC injection and decreased to 30 % over the course of the experiment, due to the warming of the chamber and the dilution of the chamber air by the replacement flow. It is known
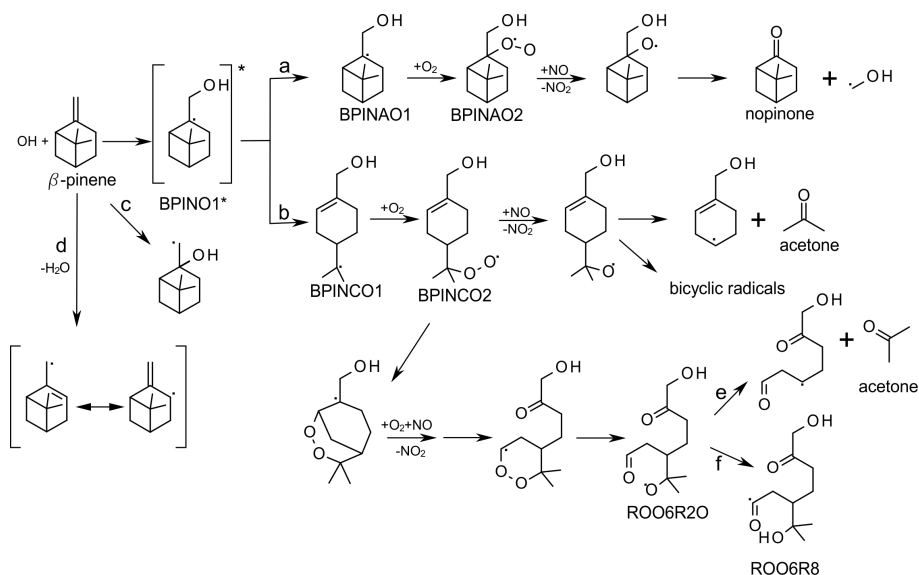
Figure 1. Acetone and nopinone formation from OH-initiated β-pinene oxidation after Vereecken and Peeters (2012). For simplification only the major reactions are shown.

for many VOC species that the product yields depend on the VOC to NO ratio (Atkinson, 2000). This is why in the two β-pinene experiments without, and the β-pinene with, the addition of 50 ppb ozone are handled separately. During the experiment on 27 August the nopinone yield as well as the acetone yield subsequently increased with the second and third β-pinene addition and are therefore denoted as range. The specified errors consider the errors of measurement of the correlated VOC concentrations as well as the errors originating from the correction of reactive losses, dilution and chamber sources. To reduce the influence of secondary product formation and to facilitate the comparability of the results, only the data of the experiment when less than 70 % of β-pinene had reacted were used for the yield calculation. To our knowledge, these are the first acetone and nopinone yields measured for reaction mixtures with less than 5 ppb of β-pinene.

Within the calculated error the determined nopinone yield in this work agrees well with every literature value except the published yield of Hatakeyama et al. (1991). These authors report nopinone yields a factor of 3 higher than every other literature value. Vereecken and Peeters (2012) pointed out that Hatakeyama et al. (1991) measured the nopinone yield by using Fourier transform infrared (FTIR) absorption at $1740\,\mathrm{cm}^{-1}$, which includes the absorption of other carbonyl compounds. Taking recent literature and our results into account it seems that the nopinone yield of β-pinene oxidation with OH does not have a strong dependence on the NO level (see Table 3). The slight increase in the nopinone yield over the three β-pinene injections in the experiment of 27 August 2012 can be related to a change of boundary conditions as well as a secondary nopinone source. For example,

the MCM 3.2 contains nopinone formation pathways from the degradation of the related hydroperoxides and organic nitrates.

The determined acetone yield is in agreement with the reported literature values of Wisthaler et al. (2001), Librando and Tringali (2005), and Larsen et al. (2001). All reported literature values are smaller than the determined acetone yields in SAPHIR and show a wide range. Similar to nopinone there is no clear evidence of an NO dependence of the acetone yield. Due to the long reaction time the increase in the acetone yield in the experiment of 27 August 2012 is most likely related to secondary acetone production. Since the yields in the literature were determined under various boundary conditions (e.g., light source, OH source, relative humidity), it is not possible to determine the reasons for the discrepancy. It could be related to different boundary conditions or measurement errors.

3.2 Comparison of trace-gas measurements with the MCM 3.2 model calculations

In this section the measured trace-gas concentrations of the β-pinene experiment from 27 August are compared to the base model using the unmodified MCM 3.2 (see Fig. 2). From the moment the roof of the SAPHIR chamber was opened, HONO was formed at the chamber walls. Due to the photolysis of HONO, OH and NO were produced in the chamber, leading to a rise in the OH as well as the NO concentration. The parameterized HONO source sufficiently describes the measured nitrogen oxides in the zero-air phase. The rise in the NO and NO_2 concentration is well captured. The modeled OH concentration also agreed well with the measurements.

Table 3. Product yields from the reaction of β-pinene with OH radicals under various NO and VOC concentrations

Product	Yield OH reaction	Reference	Consumed VOC ppbv	NO ppbv
Nopinone	0.35 ± 0.13	This work	3	0.4
	$0.28–0.37 \pm 0.13$		3	0.1
	$0.79^* \pm 0.08$	Hatakeyama et al. (1991)	700	1800
	0.30 ± 0.045	Arey et al. (1990)	960	960
	0.27 ± 0.04	Hakola et al. (1994)	1000	9600
	0.25 ± 0.05	Larsen et al. (2001)	1300–1600	0
	0.25 ± 0.03	Wisthaler et al. (2001)	1000–3000	1000–2000
	0.24	Librando and Tringali (2005)	4100–13 200	0
Acetone	0.19 ± 0.06	This work	3	0.4
	$0.20–0.36 \pm 0.07$		3	0.1
	0.13 ± 0.02	Wisthaler et al. (2001)	1000–3000	1000–2000
	0.11 ± 0.03	Larsen et al. (2001)	1300–1600	0
	0.03–0.06	Fantechi (1999)		
	0.02 ± 0.002	Orlando et al. (2000)	1800–12 000	800–8000
	0.085 ± 0.018	Reissell et al. (1999)	880–920	9600
	0.14	Librando and Tringali (2005)	4100–13 200	0

* Yield measured by FTIR absorption at $1740\,\text{cm}^{-1}$.

Besides HONO, formaldehyde, acetaldehyde and acetone were also formed or released from the chamber walls, as can be seen in the case of acetone as a slight concentration rise. These oxygenated VOC species (OVOCs) contributed to the increase in the measured background OH reactivity of $1.5\,\text{s}^{-1}$ during the zero-air phase of the experiment. As the sum of the measured OH reactants was not sufficient to explain the measured OH reactivity ($0.7\,\text{s}^{-1}$ unexplained), the modeled OH reactivity was adjusted by a constant source of a species Y, assumed to react like CO, i.e., with a similar rate coefficient and HO_2 formation. Under the assumption of a constant concentration of 120 ppb Y, the measured background reactivity is well reproduced by the model. The concentration of OH is well reproduced by MCM in the zero-air phase, while HO_2^* is slightly overestimated and RO_2^* is underestimated by 25 %. These deviations are probably caused by the chemistry of the unknown species, which contributes about half of the OH reactivity before β-pinene is injected.

With the beginning of the VOC phase of the experiments, the OH reactivity is dominated by known reactants, and good model-to-measurement agreement is expected for the radical concentrations, if the chemistry of the reactants is well understood. The reactants CO and CH_4, for example, give agreement better than 15 % for experiments in the SAPHIR chamber (Fuchs et al., 2013).

For the current case, the addition of β-pinene led to a sharp increase in the measured OH reactivity. Directly after the β-pinene injection the increase in the modeled OH reactivity, calculated from the canister injection, corresponded well with the measured $k(\text{OH})$ increase. The β-pinene concentration measured by PTR-TOF-MS was about 15 % lower than the calculated injection but still agreed with the canister injection within the instrumental uncertainty. Over the course of the VOC phase, and thereby the consumption of β-pinene, the measured OH reactivity was increasingly overestimated by the model. During this time period nopinone has the highest proportion of modeled OH reactivity besides β-pinene. However, the measured nopinone concentration was overestimated by a factor of 3 by MCM 3.2, whereas the acetone and CO concentrations were underestimated by a factor of 2. In general the MCM gives a poor description of the first-generation β-pinene degradation products. Simultaneously with the increase in the OH reactivity, a sharp decrease of the OH radical concentration was observed. At the time, the β-pinene injection model and measurement agreed well, but over the course of the experiment OH was increasingly underestimated by the model (30–50 %). The modeled concentration of theoretically measurable RO_2 radicals RO_2^* exceeded the measured concentration by about 40 %. Similar to OH, the modeled HO_2^* concentration initially agreed well with the measurements directly after β-pinene injection but was increasingly underestimated by the MCM in the latter part of the experiment. The measured time series of ozone was well captured by the MCM 3.2, whereas from the moment β-pinene was injected the model slightly overestimated the measured concentrations of HCHO, NO and NO_2.

3.3 Experimental OH budget analysis

In the OH budget analysis, the total OH production rate (P_{OH}) is compared to the OH destruction rate (D_{OH}). Both rates (P_{OH} and D_{OH}) were calculated from measurements performed during the experiments. P_{OH} is the sum of pro-
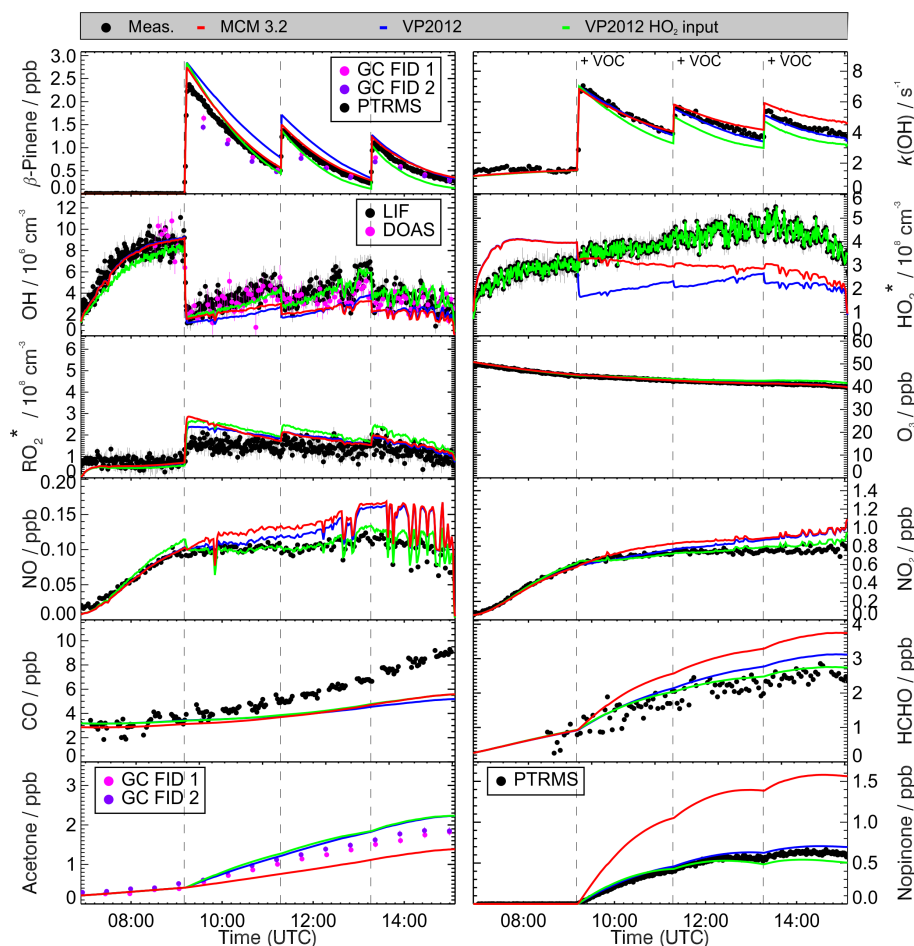
Figure 2. Comparison of the measured and modeled time series of β-pinene, k(OH), OH, HO_2^*, RO_2^*, NO, NO_2, CO, HCHO, acetone and nopinone in the β-pinene oxidation experiment from 27 August. Red: MCM 3.2. Blue: modified MCM model by Vereecken and Peeters (2012) with changed product yields. Green: modified MCM model by Vereecken and Peeters (2012) constrained by the measured HO_2 concentration.

duction rates of all known OH sources in the β-pinene experiments in SAPHIR: the photolysis of ozone and HONO, VOC ozonolysis, plus the OH production by the reaction of HO_2 with NO and O_3.

$$P_{OH} = j_{O(^1D)}[O_3] \cdot 2 f_{OH} + j_{HONO}[HONO]$$
$$+ \alpha k_1[VOC][O_3] + k_2[HO_2][NO]$$
$$+ k_3[HO_2][O_3], \qquad (8)$$
$$D_{OH} = k(OH) \cdot [OH], \qquad (9)$$

where $j_{O(^1D)}$ and j_{HONO} are the measured photolysis frequencies of O_3 and HONO, f_{OH} is the fraction of $O(^1D)$ reacting with water to OH and α defines the OH yield of β-pinene ozonolysis. The OH destruction, D_{OH}, is given by the product of the measured OH reactivity and the measured OH concentration. As the short-lived OH is in a steady state, D_{OH} should be balanced by the calculated P_{OH}, if all relevant OH source terms are included in P_{OH}.

Figure 3 displays the measured OH budget of the β-pinene experiment on 27 August 2012. The lower panel of the plot shows the time series of the calculated OH turnover rates. The OH destruction rate, D_{OH}, is given as a black line. The OH production rate, P_{OH}, is shown by the sum of the colored areas. Because of the higher instrumental accuracy the OH concentration measured by the DOAS instrument was used to calculate D_{OH}. For P_{OH} the OH recycling reaction of HO_2 with NO is the dominant OH production term followed by the photolysis of HONO. The OH production by the ozonolysis reaction of β-pinene is of minor importance. As mentioned in the previous section HO_2 measurements include an interference from specific RO_2. For the calculation of the measured OH budget HO_2 data were not corrected for an RO_2 interference, as additional sensitivity studies showed that the results of the budget analysis are not affected by an assumed RO_2 cross sensitivity of 25 %, because the derived HO_2 concentration would be lowered by less than 10 %. The upper panel of Fig. 3 shows the time series of the ratio of D_{OH}/P_{OH} (red

line). The maximum systematic error of D_{OH}/P_{OH} is indicated by the gray area. Over the course of the experiment the measured OH destruction rate is balanced by the sum of the quantifiable OH production terms within the maximum systematic error as calculated from the sum of the uncertainties of the individual measurements. Therefore, the existence of a significant unknown OH source can be excluded in the degradation of β-pinene under the experimental conditions. This result is different than previous studies of the photooxidation of isoprene and methacrolein in SAPHIR, where the same experimental setup and similar experimental conditions were applied as in the β-pinene experiments. In the case of isoprene and methacrolein, the OH budget analysis revealed significant additional OH sources (Fuchs et al., 2013, 2014), which were linked to OH regeneration by unimolecular reactions of RO_2 and contributed as much OH as the other OH production mechanisms together. To assure the quality of the measured data used for the evaluation of the OH budget, test experiments were performed in SAPHIR with CO or CH_4 as the main OH reactants. These experiments were performed before and after the β-pinene experiments and showed a balance between P_{OH} (Eq. 8) and D_{OH} (Eq. 9), as is expected for the well-known CO and CH_4 chemistry.

3.4 Modifications of the β-pinene oxidation mechanism

3.4.1 The β-pinene oxidation mechanism by Vereecken and Peeters

As discussed in Sect. 3.1 (see Table 3) and 3.2, the primary product yields of acetone and nopinone, calculated by the MCM 3.2, are not in agreement with the determined product yields under low-NO conditions in SAPHIR or with yields reported in the literature. For further evaluation of radical chemistry processes a good reproduction of the first-generation β-pinene products is essential. In the MCM 3.2 mechanism the OH radicals initially add onto the double bonds of β-pinene (reactions a, b and c in Fig. 1). About 85 % of the molecules are transformed into the tertiary radical BPINAO1. These radicals add oxygen and form the peroxy radical BPINAO2 (MCM specific designation), which reacts to nopinone. Acetone is a product of a minor pathway in which the four-membered ring of β-pinene is broken and BPINCO2 is formed (reaction b in Fig. 1). An alternative model was published by Vereecken and Peeters (2012). Nevertheless, the addition of OH to the external carbon of the double bond forming BPINO1∗ is the main reaction. However, in contrast to MCM 3.2 Vereecken and Peeters (2012) proposed a fast ring opening of BPINAO1∗ based on quantum chemical and theoretical kinetic calculations. This adjustment reduces the formation of the stabilized alkyl peroxy radical BPINAO2, the main precursor in the MCM model for nopinone formation, by about 70 %. Instead of BPINAO2 as in the MCM 3.2 mechanism, BPINCO2 is the dominant alkyl peroxy radical. With BPINCO2 as a starting point Vereecken
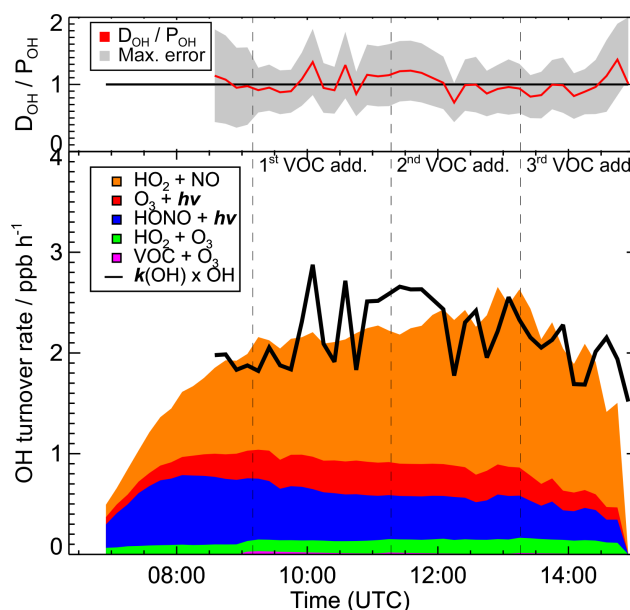

Figure 3. OH budget for the experiment on 27 August 2012. The OH destruction rate D_{OH} calculated from the measured OH reactivity k(OH) and the measured OH concentration (DOAS) is given as a black line. The colored areas display the OH production rate P_{OH} calculated from measurements. The upper panel of the diagram shows the ratio of D_{OH}/P_{OH} as a red line. The maximum systematic error of the ratio is indicated by the gray area. For reasons of clarity all data in the upper as well as the lower panel of the diagram are shown as 5 min average values. During the course of the experiment the OH destruction rate is balanced by the sum of the measurable OH production terms. The reaction of HO_2 with NO and the photolysis of HONO are the dominant OH production terms. HO_2 measurements were not corrected for the interference from specific RO_2 species.

and Peeters developed a new degradation scheme for this branch of the β-pinene oxidation. This leads to an increase in acetone formation at low NO concentrations compared to the MCM 3.2, while the yield of nopinone is predicted to be lower in the model by Vereecken and Peeters (2012). The model of Vereecken and Peeters (2012) was used without further changes except for the rate constant of β-pinene with OH, which was set to the MCM 3.2 value to facilitate model intercomparison. The original rate constant in the Vereecken and Peeters model refers to the published rate constant of Gill and Hites (2002) which is approximately 10 % lower. In the following, the MCM with the revised β-pinene mechanism of Vereecken and Peeters (2012) is denoted as VP2012. The result of the model calculation is shown in Fig. 2 as a blue line. In comparison to the MCM 3.2 the alternative β-pinene degradation scheme describes the measured time series of k(OH) better, assuming β-pinene products with a lower OH reactivity. The time behavior of the nopinone concentration is reproduced well by the Vereecken and Peeters model. The acetone formation which was slightly underesti-

mated by MCM 3.2 is now overestimated by nearly the same amount. It should be noted that the acetone formation in the model by Vereecken and Peeters depends on the fate of the radical ROO6R2O. This radical can either release acetone or undergo a hydrogen shift to yield radical ROO6R8. Unfortunately, Vereecken and Peeters could not predict the branching of these reactions accurately and were only estimating that acetone cleavage is the dominant reaction. Nevertheless, Vereecken and Peeters explicitly highlight acetone formation in the current reaction conditions as a valuable metric to verify this branching ratio. The current implementation assumes 100 % acetone formation; a more balanced value of 65 % would bring the acetone yield in agreement with the experiments.

Table 4 further illustrates the difference of the product yields for acetone and nopinone calculated by the measured and modeled time series. To enable an intercomparison the product yields calculated by modeled time series were also normalized to a β-pinene conversion of 70 %. All the corrections applied to the measured time series were applied in the same way to the modeled data. The measured nopinone yield of the first β-pinene injection is about 20 % lower than the nopinone yield observed for the second and third injection. This feature is well described by the MCM model even though the total nopinone yield is too high by approximately a factor of 2. The reason for the increase in the nopinone model yield is the secondary nopinone production by the degradation of previously formed hydroperoxides and organic nitrates originating from the same RO_2 radical which is also responsible for nopinone formation. In contrast to the MCM 3.2 the model of Vereecken and Peeters predicts a more stable nopinone yield. However, it does not include all secondary chemistry.

Over the three injections the measured acetone yield increased from 20 to 36 %, showing clear evidence for secondary acetone production. The MCM 3.2 and the Vereecken and Peeters model also show an increasing acetone yield over time. In the MCM 3.2 the acetone yield is much too low compared to the measurements but increases by a factor of 3 during the course of the experiment due to secondary acetone formation. The acetone yield calculated by the Vereecken and Peeters model for the first injection is 70 % higher than the measured value. In contrast to the time behavior of the measured values, the acetone yield is only slightly rising over the three injections, again possibly due to omitted secondary chemistry.

Concerning the agreement between measured and modeled radical concentrations, the application of the Vereecken and Peeters model does not lead to an improvement (see Fig. 2). The measured OH and HO_2^* concentrations are still underestimated in the VOC phase of the experiment. For HO_2^* the decrease after the first β-pinene injection is even more pronounced. The reason for that is the RO_2 interference included in the modeled HO_2^* data. In the Vereecken and Peeters model fewer first-generation RO_2 radicals, formed by

the oxidation of β-pinene by OH, can be theoretically detected by the LIF system. That is why directly after the first β-pinene injection the modeled observable RO_2 concentration by the Vereecken and Peeters model is lower than in MCM 3.2. Simultaneously, this also means that the modeled RO_2 interference on the HO_2^* time series is reduced. Compared to the measured time series of RO_2^*, the Vereecken and Peeters model still overestimates the measured RO_2^* concentration. The behavior of modeled NO, NO_2, CO and O_3 is similar to the MCM 3.2: NO and NO_2 concentrations are slightly overestimated by the model, CO is increasingly underestimated over time and ozone is well captured.

In summary, it can be said that the alternative β-pinene degradation mechanism of Vereecken and Peeters is able to describe the measured time series of nopinone, the measured OH reactivity and with that the OH losses during the experiment much better than the MCM 3.2. However, these improvements do not lead to a satisfying description of the measured radical concentrations by the model, and OH and HO_2^* are still underestimated.

The good reproduction of the total OH loss together with the underestimation of OH and HO_2^* by the model implies the need for an additional radical source to increase the modeled OH and HO_2 concentration. On the other hand, the OH budget analysis clearly showed that the measurable OH sources were able to balance the measured total OH loss in the experiment. With this additional information of the previous OH budget analysis, indicating no significant missing OH source, there is the arising question of how the radical production can be increased without overbalancing the OH budget. One option for that is the addition of an HO_2 source.

3.4.2 Oxidation mechanism by Vereecken and Peeters with measured HO_2^* as model input

To investigate the influence of an additional HO_2 source, another model run was performed using the VP2012 mechanism and the measured HO_2^*, taken data as model input. The known RO_2 interference in the measured HO_2^* data was taken into account and corrected in the HO_2 model input. The result of the model run is displayed by the green curve in Fig. 2. Applying an additional HO_2 source to the model improves the agreement of the modeled OH concentration with the measured values. In general the modeled OH increases by about 50 %. The higher OH level leads to an increase in chemical conversion over time, which is visible in a stronger decrease of β-pinene, nopinone, and $k(OH)$, as well as in an increase in the modeled RO_2^* concentration. Measured β-pinene, nopinone and $k(OH)$ are now underestimated by the model. A reason for that can be an underestimated RO_2 interference assumed for the HO_2 data, leading to a too-strong HO_2 source in the model. In the case of the OH reactivity there is the additional uncertainty of the OH rate constants for the assumed β-pinene oxidation products besides nopinone, potentially causing a disagreement of modeled and measured

Table 4. Comparison of measured and modeled product yields from the reaction of β-pinene with OH radicals for the three β-pinene injections during the experiment on 27 August 2012.

Product	Injection	Yield measured	Yield MCM 3.2	Yield Vereecken and Peeters
Nopinone	First	0.28	0.53	0.27
	Second	0.37	0.61	0.28
	Third	0.35	0.65	0.30
Acetone	First	0.20	0.07	0.37
	Second	0.24	0.16	0.47
	Third	0.36	0.21	0.49

$k(\text{OH})$. For the overestimation of the measured RO_2^* concentration one also has to take into account that the displayed time series of modeled RO_2^* reflects the maximum RO_2 concentration which is theoretically detectable by LIF. An overestimation of the measured RO_2^* concentration by the model might be related to an overestimation of the theoretically detectable RO_2 species in the model or an incomplete conversion of β-pinene-derived RO_2 radicals in the RO_x cell of the LIF system. In addition, the increase in the modeled HO_2^* concentration leads to an improved description of the measured NO and NO_2 time series. Especially in the second half of the VOC phase the modeled NO and NO_2 concentration is reduced. Additionally, the time series of HCHO is improved, whereas CO remains unchanged and is still underpredicted by the model. As in any other model run there is no influence on the modeled ozone time series.

Through the application of an HO_2 source to the model it was shown that the agreement between the model and measurement could be improved for important key species like OH, NO and NO_2. Discrepancies in the OH lifetime and the RO_2^* concentration could be attributed to uncertainties of the model. Therefore, a missing source of HO_2 in the degradation mechanism of β-pinene seems to be a reasonable hypothesis.

3.4.3 Uncertainties in the measured OH concentration

As stated in the previous section, the input of the measured HO_2 concentration led to a satisfactory description of the measured OH concentration by the model. On the other hand, the elevated OH concentration also resulted in an overestimated decrease of the β-pinene concentration measured by PTR-TOF-MS. From the decay of β-pinene, an OH concentration can be calculated using a reaction rate coefficient of $7.95 \times 10^{-11}\,\text{cm}^3\,\text{s}^{-1}$ (MCM v3.2) and taking dilution in the chamber into account. The calculated OH concentration is about 31 % lower than measured by the LIF and 24 % lower than measured by the DOAS instrument. Since both direct OH measurements agree well with each other and the decay of β-pinene measured by PTR-TOF-MS agrees well with the decay measured by GC/MS/FID, there is no clear indication of an instrumental failure or interference which

would lead to an exclusion of either dataset. Because this contradiction cannot be solved, the implications of a potentially lower OH concentration on the previously discussed results should be elucidated. For the OH budget analysis a 24 % lower OH concentration would lead to a decrease of the calculated OH destruction (D_{OH}) by an equal percentage. D_{OH} would be overbalanced by P_{OH}, but the mean ratio $D_{\text{OH}}/P_{\text{OH}}$ would still not be significantly different from unity, as can be seen from its experimental error (see Fig. 3, upper panel). As reported by Nehr et al. (2014) for OH budgets during SAPHIR chamber experiments investigating CO as reference system, uncertainties of $\pm 20\,\%$ for $D_{\text{OH}}/P_{\text{OH}}$ are common. For the comparison of the measured OH concentration with the model calculations, a 24 % lower measured OH concentration would result in a reduced underestimation of the measured OH concentration by the models of only 5–25 %, whereas HO_2^* would still be underestimated by a factor of 2. Consequently, taking the corrected HO_2 concentration as model input would result in an overestimation of the OH concentration by the model of up to 50 %. The influence of a 24 % lower measured OH concentration on the determined product yields would be negligible because the corrections were nevertheless small.

3.5 Possible reasons for the underestimation of HO_2^*

3.5.1 Field observations

The model simulations in the previous section demonstrated that an unaccounted source of HO_2 is a probable explanation for the disagreement of measured and modeled HO_x concentrations. A comparison of the acquired results from the SAPHIR experiments with recent field campaigns shows qualitatively the same results as in field studies which were conducted in forested areas dominated by monoterpene emissions. Kim et al. (2013) reported a mismatch of the observed HO_2 concentration and model calculations. As in the SAPHIR experiments the OH budget was nearly balanced. Kim et al. postulated a missing photolytic HO_2 source as the reason for the discrepancy between the measured and modeled HO_2 concentration in a 2-methyl-3-buten-2-ol (MBO)-dominated environment. Further investigations of the radical

budget by Wolfe et al. (2014) came to the same result. In addition to the missing HO_2 source previously postulated by Kim et al. (2013), Wolfe et al. (2014) also suggested a second peroxy radical source by the ozonolysis of unidentified VOC species, independent of photolysis. Similar to Wolfe et al. and Kim et al. (2013), Hens et al. (2014) also reported that they found an unaccounted primary HO_2 source when they were comparing the measured time series of OH and HO_2 with model calculations. Under conditions of moderate observed OH reactivity and high actinic flux, an additional RO_2 source was needed to close the radical budget. Additionally, also in the case of Hens et al. (2014), the measured OH budget was nearly balanced. In general it seems that the radical chemistry in a monoterpene-dominated biogenic atmosphere in field campaigns or chamber studies, recent atmospheric models underpredict the HO_2 production.

3.5.2 Model sensitivity studies

From the present study, it is obvious that an unknown HO_2 source is linked to the oxidation of β-pinene. Further model studies were performed to identify possible mechanisms that could generate additional HO_2. In atmospheric chemistry, primary sources of HO_2 include the photolysis of aldehydes and ketones as well as the ozonolysis of VOCs. Furthermore, HO_2 is produced by the reaction of CO, ozone or formaldehyde with OH. In the chemical degradation of VOCs, HO_2 can be formed by the decomposition of alkoxy radicals and finally by unimolecular rearrangement reactions of alkyl peroxy radicals (Orlando and Tyndall, 2012). We have investigated two potential sources of HO_2 in separate model runs: firstly, the formation of HO_2 by photolysis of β-pinene reaction products, in particular aldehydes and ketones, and secondly the additional conversion of RO_2 to HO_2 without the involvement of NO. In both cases, generic reactions were added to the chemical mechanism (see details in the Supplement). In the case of the photolytical source, it was assumed that every reaction of β-pinene with OH produces one molecule of a carbonyl-type species Z in addition to the related RO_2 species. It was further assumed that Z is photolyzed with a rate similar to formaldehyde and generates six HO_2 and CO molecules per molecule of Z, which is in terms of chemical feasibility a rather unlikely, but not impossible, assumption (see Supplement). Based on these assumptions, agreement between the measurement and model is found for HO_2^* and OH in the second half of the VOC phase, but in the first half of the VOC phase a strong underestimation of HO_2^* remains (Fig. S1, Supplement). Compared to all previous model runs, the measured concentration of CO is now well matched by the model. The modeled time series of RO_2, NO, NO_2, ozone and the β-pinene products formaldehyde, acetone and nopinone stay nearly unchanged in comparison to the model run using measured HO_2 as model input. In conclusion, the assumed photolytical HO_2 source gives an improved model description of the observations but is not

capable of regenerating HO_2 fast enough in the first 1–2 h after the first β-pinene addition.

Next, the possible influence of unimolecular rearrangement of RO_2 yielding HO_2 was studied (see Supplement). For this purpose, the so-called X mechanism published by Hofzumahaus et al. (2009) was used. An NO-like species X is thereby reducing RO_2 radicals to RO radicals. The rate constants applied for these reactions are the same as the rate coefficients of NO with the corresponding RO_2 radical. Contrary to the X mechanism of Hofzumahaus et al., in the case of β-pinene, X is not reacting with HO_2 radicals. With 300 pptv of X, the model gives a significantly improved description of HO_2^*, but an underprediction of 25 % remains (Fig. S1, Supplement). The introduction of X causes a substantial decrease in RO_2^* and a significant overprediction of NO and NO_2 by the model. Additionally, CO is greatly overestimated. In conclusion, the additional RO_2 to HO_2 conversion (without NO) alone is not capable of describing all the observations consistently.

Two additional model sensitivity tests were carried out in order to investigate if the HO_2^* underprediction is caused by too-fast $RO_2 + HO_2$ reactions in the Vereecken and Peters model and how the model measurement comparison is influenced by uncertainties of the RO_2 interference in the HO_2 measurements (see details in Supplement).

In accordance with a proposed uncertainty of a factor of 2 for the rate constants of biogenic $RO_2 + HO_2$ reactions (Orlando and Tyndall, 2012), the rate constants for the formation of ROOH were reduced by 50 %. As a result the modeled HO_2 concentration increases by 30 %, but HO_2 is still underestimated by the model (Fig. S1, Supplement). The modeled OH concentration slightly increases and the measured RO_2 concentration becomes overestimated by a factor of 2. The measured concentrations of NO and NO_2 are well matched by the model, but CO remains underestimated. In conclusion, a reduction of the ROOH production may help to reduce the discrepancy between the modeled and measured HO_2 concentration but cannot solely explain the deviations between the model and measurements. As the interference of RO_2 radicals in the measurements of HO_2 is also a subject of discussion, the maximum influence of the assumed RO_2 interference on the model results was estimated in a fourth model case (see Supplement). The sensitivity study proved that the interference of the RO_2 radicals on the measured HO_2 time series is not able to explain the observed deviations between modeled and measured HO_2. More than 50 % of the observed discrepancy cannot be explained by any known interference.

3.5.3 Modifications of the β-pinene oxidation mechanism by Vereecken and Peeters to explain the missing HO_2^* source

The major difference between the β-pinene oxidation mechanism by Vereecken and Peeters and the MCM 3.2 mechanism is the fast ring opening of the alkoxy radical BPINO1* which
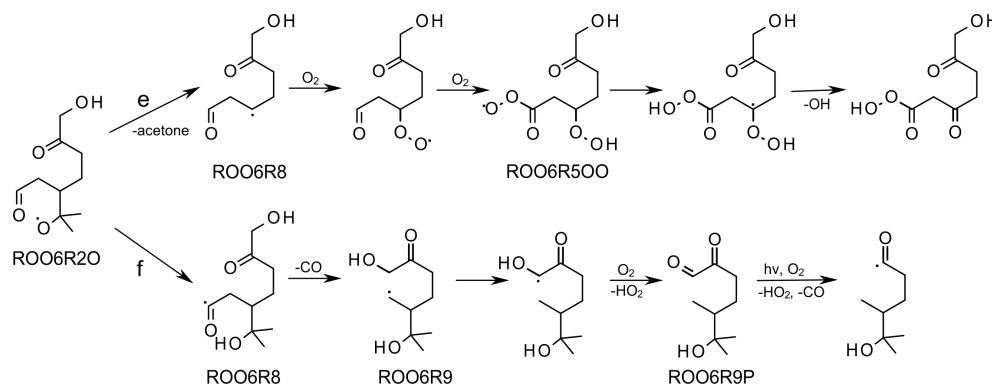
Figure 4. Possible HO_2 formation pathway in the oxidation of β-pinene modified after Vereecken and Peeters (2012).

is transformed into the radical BPINCO1 (see Fig. 1). At low NO concentrations the largest fraction of these molecules are expected to react to ROO6R2O. The formation of ROO6R2O is exothermic, and the reaction sequence can either proceed via elimination of acetone (path e in Figs. 1 and 4) or via 1,5-H migration of the hydrogen at the α position of the aldehyde (path f in Fig. 1 and in Fig. 4).

The branching ratio of path e and path f significantly influences the amount of HO_2 produced. After acetone is eliminated ROO6R8 radicals add two oxygen molecules. The emerged radical cleaves an OH radical and forms a peracid. No additional HO_2 radicals are supposed to be produced if degradation of the radical ROO6R2O proceeds via the acetone elimination channel.

If the hydrogen atom on the α position of the aldehyde of ROO6R2O migrates instead, ROO6R8 is formed. This acyl radical is supposed to cleave CO and, after another 1,5-H migration, also HO_2. The resulting molecule is the dicarbonyl compound ROO6R9P, whose photolytic cleavage results in the additional production of one molecule CO and one molecule HO_2 (path f in Fig. 4). Unfortunately, Vereecken and Peeters could not accurately predict the branching ratio of these two reaction channels due to the large number of active conformers at higher energies. Instead, the 1,5-H migration in path f was supposed to be outrun by acetone elimination in path e, and path f was omitted in the model of Vereecken and Peeters.

The effect of the branching ratio in Fig. 4 on the predicted HO_2^* concentration can be evaluated if ROO6R2O is fixed in the model to react exclusively via path f. The respective model run (see the green curve in Fig. 5) predicts an HO_2^* concentration which is 30 % higher than forecasted by the original model of Vereecken and Peeters. Additionally, the predicted CO, RO_2^*, HCHO and nopinone concentrations now coincide with the measured data. Nevertheless, the measured HO_2^* is 20 % higher than anticipated.

The gap between measured HO_2^* and modeled HO_2^* can be closed if the cleavage of a second HO_2 and a second CO is incorporated into the model (see the orange curve in Fig. 5).

The time series of HO_2^*, RO_2^* and OH are now captured by the model. Additionally, the measured nopinone, CO and HCHO are well described. Only acetone is now underestimated by the model, because acetone is mainly formed via pathway e in Fig. 4. Although ROO6R9P can potentially cleave acetone, quantum chemical calculations are needed to further pin down the mechanism of acetone cleavage.

4 Summary and conclusions

A set of three β-pinene oxidation experiments, conducted in the SAPHIR atmosphere simulation chamber, was comprehensively investigated with regard to the involved radical species during the OH oxidation. A special focus was placed on the identification of possible missing OH production terms in the degradation mechanism (Whalley et al., 2011). The experiments were conducted under nearly ambient β-pinene concentration (4.3–4.7 ppb VOC) and low-NO conditions (100–300 ppt NO). The comparatively low VOC concentration allowed for the first time the investigation of the radical budget of β-pinene by parallel measurements of OH, HO_2, RO_2 and $k(OH)$. In a first approach this comprehensive dataset was used for a model-independent analysis of the OH budget. For this purpose the sum of the measurable OH production terms (HONO photolysis, O_3 photolysis, VOC ozonolysis, HO_2 + NO, HO_2 + O_3) was compared with the measured OH destruction rate ($k(OH) \times$ [OH]). Contrary to previous studies of isoprene and methacrolein in SAPHIR (Fuchs et al., 2013, 2014), the OH budget was balanced in the β-pinene oxidation experiments, giving no evidence for significant missing OH production terms. In a second approach the measured time series of the atmospheric key species were compared to zero-dimensional box model calculations to investigate whether the models are able to predict the β-pinene degradation well. The comparison of the measured time series with the MCM 3.2 revealed that the model was not able to reproduce the measured time series of OH, HO_2, $k(OH)$ and nopinone. The modeled OH as well as the HO_2 concentration was underestimated by more

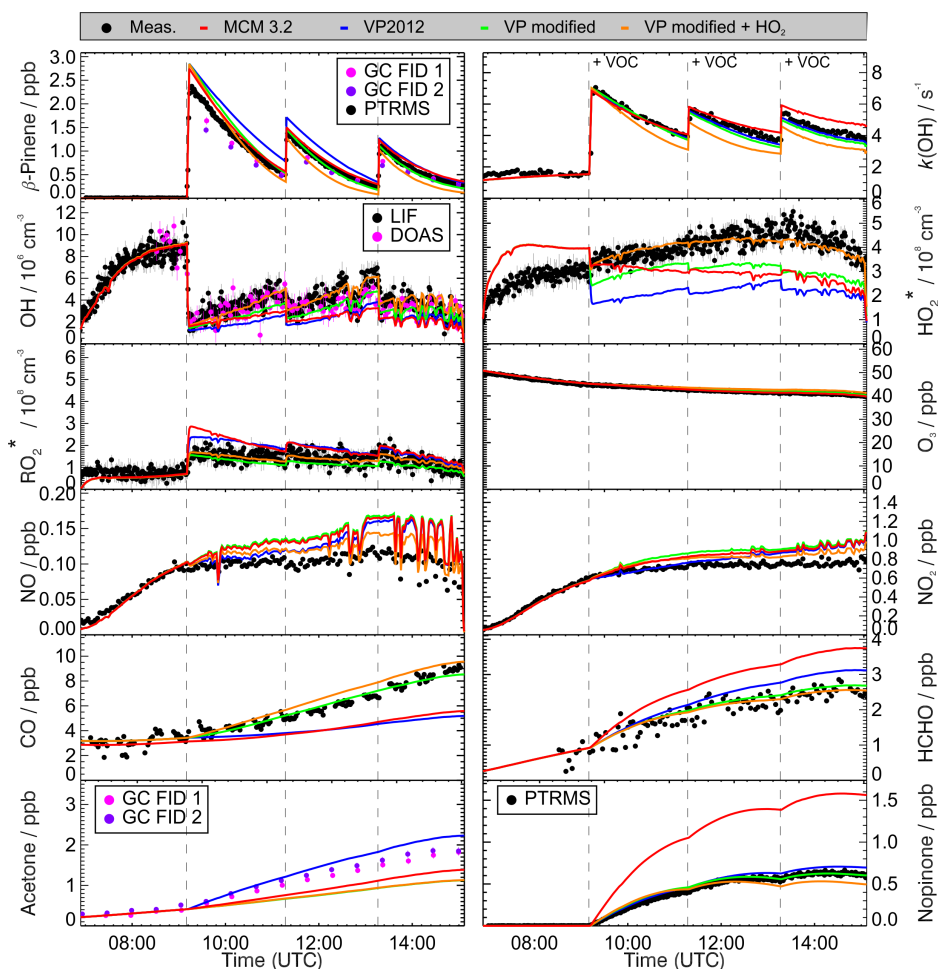**Figure 5.** Comparison of the measured and modeled time series of β-pinene, OH, OH, HO_2^*, RO_2^*, NO, NO_2, CO, HCHO, acetone and nopinone in the β-pinene oxidation experiment from 27 August. Red: MCM 3.2. Blue: model by Vereecken and Peeters (2012). Green: model by Vereecken and Peeters (2012) with 1,5-H migration of ROO6R2O. Orange: modified model by Vereecken and Peeters (2012) with 1,5-H migration of ROO6R2O and an additional production term for one molecule of HO_2 and CO.

than 50 %. At the same time the modeled OH reactivity was slightly overestimated. The reason for this disagreement is obviously a biased product distribution of the first-generation degradation products. The measured nopinone concentration was about a factor of 3 lower than predicted by the model. A comparison of the experimentally determined nopinone yield with recent literature showed a good agreement but is a factor of 2 lower than in the MCM model. Hence, for further investigations an updated MCM mechanism published by Vereecken and Peeters (2012) was used. Their model was able to reproduce the measured time series of nopinone and k(OH) much better than the MCM 3.2 but still significantly underpredicted the measured OH and HO_2 concentration. As the previous analysis of the OH budget showed no evidence of a missing OH source, an additional HO_2 source was introduced into the model to improve the agreement for OH and HO_2. A sensitivity study showed that taking the measured HO_2 time series as model input generally improves the

overall agreement of the modeled time series with the measurements. OH is now well described by the model. These findings are qualitatively in agreement with recent field studies (Kim et al., 2013; Wolfe et al., 2014; Hens et al., 2014) reporting that in a monoterpene-dominated biogenic atmosphere, models were not able to describe OH and HO_2 levels well, although the measured OH budget was balanced.

In accordance with the results for β-pinene presented in this paper we propose an additional HO_2 source linked to b-pinene oxidation products as the reason for the underestimation of OH and HO_2 in the model. With additional sensitivity studies it was possible to rule out photolytical processes or rearrangement reactions of RO_2 as the sole HO_2 sources. Additionally, a possible overestimation of the yield of organic hydroperoxides and an underestimation of the known RO_2 interference on the HO_2 measurements were excluded as explanations for underestimating HO_2 in the model.

The gap between measured and modeled HO_2^* concentration can significantly be reduced by modifying the mechanism of Vereecken and Peeters in such a way that the radical intermediate ROO6R2O is rearranged rather than cleaved. The resulting acyl radical produces HO_2, CO and a dicarbonyl compound which itself is a photolytical source of HO_2 and CO. Nevertheless, the exact HO_2 formation mechanism remains uncertain. Additional experiments and quantum chemical calculations have to be made to completely unravel the pathway of HO_2 formation.

The Supplement related to this article is available online at https://doi.org/10.5194/acp-17-6631-2017-supplement.

Competing interests. The authors declare that they have no conflict of interest.

Edited by: D. Heard
Reviewed by: two anonymous referees

References

Arey, J., Atkinson, R., and Aschmann, S. M.: Product study of the gas-phase reactions of monoterpenes with the OH radical in the presence of NO_x, J. Geophys. Res.-Atmos., 95, 18539–18546, https://doi.org/10.1029/JD095iD11p18539, 1990.

Atkinson, R.: Atmospheric chemistry of VOCs and NO_x, Atmos. Environ., 34, 2063–2101, https://doi.org/10.1016/s1352-2310(99)00460-4, 2000.

Atkinson, R. and Arey, J.: Gas-phase tropospheric chemistry of biogenic volatile organic compounds: a review, Atmos. Environ., 37, Supplement 2, 197–219, https://doi.org/10.1016/s1352-2310(03)00391-1, 2003.

Bates, K. H., Crounse, J. D., St Clair, J. M., Bennett, N. B., Nguyen, T. B., Seinfeld, J. H., Stoltz, B. M., and Wennberg, P. O.: Gas Phase Production and Loss of Isoprene Epoxydiols, J. Phys. Chem. A, 118, 1237–1246, https://doi.org/10.1021/jp4107958, 2014.

Bohn, B. and Zilken, H.: Model-aided radiometric determination of photolysis frequencies in a sunlit atmosphere simulation chamber, Atmos. Chem. Phys., 5, 191–206, https://doi.org/10.5194/acp-5-191-2005, 2005.

Bohn, B., Rohrer, F., Brauers, T., and Wahner, A.: Actinometric Measurements of NO_2 Photolysis Frequencies in the Atmosphere Simulation Chamber SAPHIR, Atmos. Chem. Phys., 5, 493–503, https://doi.org/10.5194/acp-5-493-2005, 2005.

Brauers, T., Bossmeyer, J., Dorn, H. P., Schlosser, E., Tillmann, R., Wegener, R., and Wahner, A.: Investigation of the formaldehyde differential absorption cross section at high and low spectral resolution in the simulation chamber SAPHIR, Atmos. Chem. Phys., 7, 3579–3586, https://doi.org/10.5194/acp-7-3579-2007, 2007.

Calogirou, A., Larsen, B. R., and Kotzias, D.: Gas-phase terpene oxidation products: a review, Atmos. Environ., 33, 1423–1439, https://doi.org/10.1016/s1352-2310(98)00277-5, 1999.

Carslaw, N., Creasey, D., Harrison, D., Heard, D., Hunter, M., Jacobs, P., Jenkin, M., Lee, J., Lewis, A., Pilling, M., Saunders, S., and Seakins, P.: OH and HO_2 radical chemistry in a forested region of north-western Greece, Atmos. Environ., 35, 4725–4737, https://doi.org/10.1016/S1352-2310(01)00089-9, 2001.

Crounse, J. D., Paulot, F., Kjaergaard, H. G., and Wennberg, P. O.: Peroxy radical isomerization in the oxidation of isoprene, Phys. Chem. Chem. Phys., 13, 13607–13613, https://doi.org/10.1039/C1CP21330J, 2011.

Crounse, J. D., Knap, H. C., Ørnsø, K. B., Jørgensen, S., Paulot, F., Kjaergaard, H. G., and Wennberg, P. O.: Atmospheric Fate of Methacrolein. 1. Peroxy Radical Isomerization Following Addition of OH and O_2, J. Phys. Chem. A, 116, 5756–5762, https://doi.org/10.1021/jp211560u, 2012.

Crounse, J. D., Nielsen, L. B., Jørgensen, S., Kjaergaard, H. G., and Wennberg, P. O.: Autoxidation of Organic Compounds in the Atmosphere, J. Phys. Chem. Lett., 4, 3513–3520, https://doi.org/10.1021/jz4019207, 2013.

da Silva, G., Graham, C., and Wang, Z.-F.: Unimolecular β-Hydroxyperoxy Radical Decomposition with OH Recycling in the Photochemical Oxidation of Isoprene, Environ. Sci. Technol., 44, 250–256, https://doi.org/10.1021/es900924d, 2010.

Dorn, H.-P., Brandenburger, U., Brauers, T., and Hausmann, M.: A New In Situ Laser Long-Path Absorption Instrument for the Measurement of Tropospheric OH Radicals, J. Atmos. Sci., 52, 3373–3380, https://doi.org/10.1175/1520-0469(1995)052<3373:ANISLL>2.0.CO;2, 1995.

Dorn, H.-P., Apodaca, R. L., Ball, S., Brauers, T., Brown, S., Crowley, J., Dubé, W., Häseler, R., Heitmann, U., Jones, R., Kiendler-Scharr, A., Labazan, I., Langridge, J., Meinen, J., Mentel, T., Platt, U., Pöhler, D., Rohrer, F., Ruth, A., Schlosser, E., Schuster, G., Schillings, A., Simpson, W., Thieser, J., Tillmann, R., Varma, R., Venebles, D., and Wahner, A.: Intercomparison of

NO$_3$ radical detection instruments in the atmosphere simulation chamber SAPHIR, Atmos. Meas. Tech., 6, 1111–1140, https://doi.org/10.5194/amt-6-1111-2013, 2013.

Eddingsaas, N. C., Loza, C. L., Yee, L. D., Chan, M., Schilling, K. A., Chhabra, P. S., Seinfeld, J. H., and Wennberg, P. O.: α-pinene photooxidation under controlled chemical conditions – Part 2: SOA yield and composition in low- and high-NO$_x$ environments, Atmos. Chem. Phys., 12, 7413–7427, https://doi.org/10.5194/acp-12-7413-2012, 2012a.

Eddingsaas, N. C., Loza, C. L., Yee, L. D., Seinfeld, J. H., and Wennberg, P. O.: α-pinene photooxidation under controlled chemical conditions – Part 1: Gas-phase composition in low- and high-NO$_x$ environments, Atmos. Chem. Phys., 12, 6489–6504, https://doi.org/10.5194/acp-12-6489-2012, 2012b.

Ehn, M., Thornton, J. A., Kleist, E., Sipila, M., Junninen, H., Pullinen, I., Springer, M., Rubach, F., Tillmann, R., Lee, B., Lopez-Hilfiker, F., Andres, S., Acir, I.-H., Rissanen, M., Jokinen, T., Schobesberger, S., Kangasluoma, J., Kontkanen, J., Nieminen, T., Kurten, T., Nielsen, L. B., Jorgensen, S., Kjaergaard, H. G., Canagaratna, M., Dal Maso, M., Berndt, T., Petaja, T., Wahner, A., Kerminen, V.-M., Kulmala, M., Worsnop, D. R., Wildt, J., and Mentel, T. F.: A large source of low-volatility secondary organic aerosol, Nature, 506, p. 476, https://doi.org/10.1038/nature13032, 2014.

Fantechi, G.: Atmospheric oxidation reactions of selected biogenic volatile organic compounds (BIOVOCs): A smog chamber study, PhD thesis, KULeuven, 1999.

Feiner, P. A., Brune, W. H., Miller, D. O., Zhang, L., Cohen, R. C., Romer, P. S., Goldstein, A. H., Keutsch, F. N., Skog, K. M., Wennberg, P. O., Nguyen, T. B., Teng, A. P., DeGouw, J., Koss, A., Wild, R. J., Brown, S. S., Guenther, A., Edgerton, E., Baumann, K., and Fry, J. L.: Testing Atmospheric Oxidation in an Alabama Forest, J. Atmos. Sci., 73, 4699–4710, https://doi.org/10.1175/JAS-D-16-0044.1, 2016.

Fuchs, H., Holland, F., and Hofzumahaus, A.: Measurement of tropospheric RO$_2$ and HO$_2$ radicals by a laser-induced fluorescence instrument, Rev. Sci. Instrum., 79, 084104, https://doi.org/10.1063/1.2968712, 2008.

Fuchs, H., Bohn, B., Hofzumahaus, A., Holland, F., Lu, K. D., Nehr, S., Rohrer, F., and Wahner, A.: Detection of HO$_2$ by laser-induced fluorescence: calibration and interferences from RO$_2$ radicals, Atmos. Meas. Tech., 4, 1209–1225, https://doi.org/10.5194/amt-4-1209-2011, 2011.

Fuchs, H., Dorn, H. P., Bachner, M., Bohn, B., Brauers, T., Gomm, S., Hofzumahaus, A., Holland, F., Nehr, S., Rohrer, F., Tillmann, R., and Wahner, A.: Comparison of OH concentration measurements by DOAS and LIF during SAPHIR chamber experiments at high OH reactivity and low NO concentration, Atmos. Meas. Tech., 5, 1611–1626, https://doi.org/10.5194/amt-5-1611-2012, 2012.

Fuchs, H., Hofzumahaus, A., Rohrer, F., Bohn, B., Brauers, T., Dorn, H. P., Häseler, R., Holland, F., Kaminski, M., Li, X., Lu, K., Nehr, S., Tillmann, R., Wegener, R., and Wahner, A.: Experimental evidence for efficient hydroxyl radical regeneration in isoprene oxidation, Nat. Geosci., 6, 1023–1026, https://doi.org/10.1038/ngeo1964, 2013.

Fuchs, H., Acir, I. H., Bohn, B., Brauers, T., Dorn, H. P., Häseler, R., Hofzumahaus, A., Holland, F., Kaminski, M., Li, X., Lu, K., Lutz, A., Nehr, S., Rohrer, F., Tillmann, R., Wegener, R., and

Wahner, A.: OH regeneration from methacrolein oxidation investigated in the atmosphere simulation chamber SAPHIR, Atmos. Chem. Phys., 14, 7895–7908, https://doi.org/10.5194/acp-14-7895-2014, 2014.

Fuchs, H., Tan, Z. F., Hofzumahaus, A., Broch, S., Dorn, H. P., Holland, F., Kunstler, C., Gomm, S., Rohrer, F., Schrade, S., Tillmann, R., and Wahner, A.: Investigation of potential interferences in the detection of atmospheric RO$_x$ radicals by laser-induced fluorescence under dark conditions, Atmos. Meas. Tech., 9, 1431–1447, https://doi.org/10.5194/amt-9-1431-2016, 2016.

Galloway, M. M., Huisman, A. J., Yee, L. D., Chan, A. W. H., Loza, C. L., Seinfeld, J. H., and Keutsch, F. N.: Yields of oxidized volatile organic compounds during the OH radical initiated oxidation of isoprene, methyl vinyl ketone, and methacrolein under high-NO$_x$ conditions, Atmos. Chem. Phys., 11, 10779–10790, https://doi.org/10.5194/acp-11-10779-2011, 2011.

Gill, K. J. and Hites, R. A.: Rate Constants for the Gas-Phase Reactions of the Hydroxyl Radical with Isoprene, α- and β-Pinene, and Limonene as a Function of Temperature, J. Phys. Chem. A, 106, 2538–2544, https://doi.org/10.1021/jp013532q, 2002.

Goldstein, A. H. and Galbally, I. E.: Known and Unexplored Organic Constituents in the Earth's Atmosphere, Environ. Sci. Technol., 41, 1514–1521, https://doi.org/10.1021/es072476p, 2007.

Griffith, S. M., Hansen, R. F., Dusanter, S., Stevens, P. S., Alaghmand, M., Bertman, S. B., Carroll, M. A., Erickson, M., Galloway, M., Grossberg, N., Hottle, J., Hou, J., Jobson, B. T., Kammrath, A., Keutsch, F. N., Lefer, B. L., Mielke, L. H., O'Brien, A., Shepson, P. B., Thurlow, M., Wallace, W., Zhang, N., and Zhou, X. L.: OH and HO$_2$ radical chemistry during PROPHET 2008 and CABINEX 2009 – Part 1: Measurements and model comparison, Atmos. Chem. Phys., 13, 5403–5423, https://doi.org/10.5194/acp-13-5403-2013, 2013.

Guenther, A., Hewitt, C. N., Erickson, D., Fall, R., Geron, C., Graedel, T., Harley, P., Klinger, L., Lerdau, M., McKay, W. A., Pierce, T., Scholes, B., Steinbrecher, R., Tallamraju, R., Taylor, J., and Zimmerman, P.: A global model of natural volatile organic compound emissions, J. Geophys. Res.-Atmos., 100, 8873–8892, https://doi.org/10.1029/94JD02950, 1995.

Guenther, A. B., Jiang, X., Heald, C. L., Sakulyanontvittaya, T., Duhl, T., Emmons, L. K., and Wang, X.: The Model of Emissions of Gases and Aerosols from Nature version 2.1 (MEGAN2.1): an extended and updated framework for modeling biogenic emissions, Geosci. Model Dev., 5, 1471–1492, https://doi.org/10.5194/gmd-5-1471-2012, 2012.

Hakola, H., Arey, J., Aschmann, S., and Atkinson, R.: Product formation from the gas-phase reactions of OH radicals and O$_3$ with a series of monoterpenes, J. Atmos. Chem., 18, 75–102, https://doi.org/10.1007/BF00694375, 1994.

Häseler, R., Brauers, T., Holland, F., and Wahner, A.: Development and application of a new mobile LOPAP instrument for the measurement of HONO altitude profiles in the planetary boundary layer, Atmos. Meas. Tech. Discuss., 2, 2027–2054, https://doi.org/10.5194/amtd-2-2027-2009, 2009.

Hatakeyama, S., Izumi, K., Fukuyama, T., Akimoto, H., and Washida, N.: Reactions of OH with α-pinene and β-pinene in air: Estimate of global CO production from the atmospheric oxidation of terpenes, J. Geophys. Res.-Atmos., 96, 947–958, https://doi.org/10.1029/90JD02341, 1991.

Hausmann, M., Brandenburger, U., Brauers, T., and Dorn, H.-P.: Detection of tropospheric OH radicals by long-path differential-optical-absorption spectroscopy: Experimental setup, accuracy, and precision, J. Geophys. Res.-Atmos., 102, 16011–16022, https://doi.org/10.1029/97JD00931, 1997.

Hens, K., Novelli, A., Martinez, M., Auld, J., Axinte, R., Bohn, B., Fischer, H., Keronen, P., Kubistin, D., Nölscher, A. C., Oswald, R., Paasonen, P., Petäjä, T., Regelin, E., Sander, R., Sinha, V., Sipilä, M., Taraborrelli, D., Tatum Ernest, C., Williams, J., Lelieveld, J., and Harder, H.: Observation and modelling of HO$_x$ radicals in a boreal forest, Atmos. Chem. Phys., 14, 8723–8747, https://doi.org/10.5194/acp-14-8723-2014, 2014.

Hofzumahaus, A. and Heard, D. H.: Assessment of local HO$_x$ and RO$_x$ Measurement Techniques: Achievements, Challenges, and Future Directions. Report of the International HO$_x$ Workshop 2015, Jülich, Tech. rep., Forschungszentrum Jülich, 2016.

Hofzumahaus, A., Rohrer, F., Lu, K., Bohn, B., Brauers, T., Chang, C.-C., Fuchs, H., Holland, F., Kita, K., Kondo, Y., Li, X., Lou, S., Shao, M., Zeng, L., Wahner, A., and Zhang, Y.: Amplified Trace Gas Removal in the Troposphere, Science, 324, 1702–1704, https://doi.org/10.1126/science.1164566, 2009.

Holland, F., Heßling, M., and Hofzumahaus, A.: In situ measurement of tropospheric OH radicals by laser-induced fluorescence – A description of the KFA instrument, J. Atmos. Sci., 52, 3393–3401, https://doi.org/10.1175/1520-0469(1995)052<3393:ismoto>2.0.co;2, 1995.

Jenkin, M. E., Saunders, S. M., and Pilling, M. J.: The tropospheric degradation of volatile organic compounds: A protocol for mechanism development, Atmos. Environ., 31, 81–104, https://doi.org/10.1016/s1352-2310(96)00105-7, 1997.

Jordan, A., Haidacher, S., Hanel, G., Hartungen, E., Märk, L., Seehauser, H., Schottkowsky, R., Sulzer, P., and Märk, T. D.: A high resolution and high sensitivity proton-transfer-reaction time-of-flight mass spectrometer (PTR-TOF-MS), Int. J. Mass Spectrom., 286, 122–128, https://doi.org/10.1016/j.ijms.2009.07.005, 2009.

Kaminski, M.: Untersuchung des photochemischen Terpenoidabbaus in der Atmosphärensimulationskammer SAPHIR, Forschungszentrum Jülich, 2014.

Kanakidou, M., Seinfeld, J. H., Pandis, S. N., Barnes, I., Dentener, F. J., Facchini, M. C., Van Dingenen, R., Ervens, B., Nenes, A., Nielsen, C. J., Swietlicki, E., Putaud, J. P., Balkanski, Y., Fuzzi, S., Horth, J., Moortgat, G. K., Winterhalter, R., Myhre, C. E. L., Tsigaridis, K., Vignati, E., Stephanou, E. G., and Wilson, J.: Organic aerosol and global climate modelling: a review, Atmos. Chem. Phys., 5, 1053–1123, https://doi.org/10.5194/acp-5-1053-2005, 2005.

Karl, M., Dorn, H. P., Holland, F., Koppmann, R., Poppe, D., Rupp, L., Schaub, A., and Wahner, A.: Product study of the reaction of OH radicals with isoprene in the atmosphere simulation chamber SAPHIR, J. Atmos. Chem., 55, 167–187, https://doi.org/10.1007/s10874-006-9034-x, 2006.

Kim, S., Wolfe, G. M., Mauldin, L., Cantrell, C., Guenther, A., Karl, T., Turnipseed, A., Greenberg, J., Hall, S. R., Ullmann, K., Apel, E., Hornbrook, R., Kajii, Y., Nakashima, Y., Keutsch, F. N., Di-Gangi, J. P., Henry, S. B., Kaser, L., Schnitzhofer, R., Graus, M., Hansel, A., Zheng, W., and Flocke, F. F.: Evaluation of HO$_x$ sources and cycling using measurement-constrained model calculations in a 2-methyl-3-butene-2-ol (MBO) and monoterpene

(MT) dominated ecosystem, Atmos. Chem. Phys., 13, 2031–2044, https://doi.org/10.5194/acp-13-2031-2013, 2013.

Kubistin, D., Harder, H., Martinez, M., Rudolf, M., Sander, R., Bozem, H., Eerdekens, G., Fischer, H., Gurk, C., Klüpfel, T., Königstedt, R., Parchatka, U., Schiller, C. L., Stickler, A., Taraborrelli, D., Williams, J., and Lelieveld, J.: Hydroxyl radicals in the tropical troposphere over the Suriname rainforest: comparison of measurements with the box model MECCA, Atmos. Chem. Phys., 10, 9705–9728, https://doi.org/10.5194/acp-10-9705-2010, 2010.

Larsen, B. R., Di Bella, D., Glasius, M., Winterhalter, R., Jensen, N. R., and Hjorth, J.: Gas-Phase OH Oxidation of Monoterpenes: Gaseous and Particulate Products, J. Atmos. Chem., 38, 231–276, https://doi.org/10.1023/A:1006487530903, 2001.

Lee, A., Goldstein, A. H., Keywood, M. D., Gao, S., Varutbangkul, V., Bahreini, R., Ng, N. L., Flagan, R. C., and Seinfeld, J. H.: Gas-phase products and secondary aerosol yields from the ozonolysis of ten different terpenes, J. Geophys. Res.-Atmos., 111, D07302, https://doi.org/10.1029/2005jd006437, 2006.

Lelieveld, J., Butler, T. M., Crowley, J. N., Dillon, T. J., Fischer, H., Ganzeveld, L., Harder, H., Lawrence, M. G., Martinez, M., Taraborrelli, D., and Williams, J.: Atmospheric oxidation capacity sustained by a tropical forest, Nature, 452, 737–740, https://doi.org/10.1038/nature06870, 2008.

Librando, V. and Tringali, G.: Atmospheric fate of OH initiated oxidation of terpenes. Reaction mechanism of α-pinene degradation and secondary organic aerosol formation, J. Environ. Manage., 75, 275–282, https://doi.org/10.1016/j.jenvman.2005.01.001, 2005.

Lindinger, W., Hansel, A., and Jordan, A.: On-line monitoring of volatile organic compounds at pptv levels by means of Proton-Transfer-Reaction Mass Spectrometry (PTR-MS) Medical applications, food control and environmental research, Int. J. Mass Spectrom. Ion Process., 173, 191–241, https://doi.org/10.1016/s0168-1176(97)00281-4, 1998.

Liu, Y. J., Herdlinger-Blatt, I., McKinney, K. A., and Martin, S. T.: Production of methyl vinyl ketone and methacrolein via the hydroperoxyl pathway of isoprene oxidation, Atmos. Chem. Phys., 13, 5715–5730, https://doi.org/10.5194/acp-13-5715-2013, 2013.

Lou, S., Holland, F., Rohrer, F., Lu, K., Bohn, B., Brauers, T., Chang, C. C., Fuchs, H., Häseler, R., Kita, K., Kondo, Y., Li, X., Shao, M., Zeng, L., Wahner, A., Zhang, Y., Wang, W., and Hofzumahaus, A.: Atmospheric OH reactivities in the Pearl River Delta – China in summer 2006: measurement and model results, Atmos. Chem. Phys., 10, 11243–11260, https://doi.org/10.5194/acp-10-11243-2010, 2010.

Lu, K. D., Rohrer, F., Holland, F., Fuchs, H., Bohn, B., Brauers, T., Chang, C. C., Häseler, R., Hu, M., Kita, K., Kondo, Y., Li, X., Lou, S. R., Nehr, S., Shao, M., Zeng, L. M., Wahner, A., Zhang, Y. H., and Hofzumahaus, A.: Observation and modelling of OH and HO$_2$ concentrations in the Pearl River Delta 2006: a missing OH source in a VOC rich atmosphere, Atmos. Chem. Phys., 12, 1541–1569, https://doi.org/10.5194/acp-12-1541-2012, 2012.

Mao, J., Ren, X., Zhang, L., Van Duin, D. M., Cohen, R. C., Park, J.-H., Goldstein, A. H., Paulot, F., Beaver, M. R., Crounse, J. D., Wennberg, P. O., DiGangi, J. P., Henry, S. B., Keutsch, F. N., Park, C., Schade, G. W., Wolfe, G. M., Thornton, J. A., and Brune, W. H.: Insights into hydroxyl measurements and atmo-

spheric oxidation in a California forest, Atmos. Chem. Phys., 12, 8009–8020, https://doi.org/10.5194/acp-12-8009-2012, 2012.

Nehr, S., Bohn, B., Dorn, H.-P., Fuchs, H., Häseler, R., Hofzumahaus, A., Li, X., Rohrer, F., Tillmann, R., and Wahner, A.: Atmospheric photochemistry of aromatic hydrocarbons: OH budgets during SAPHIR chamber experiments, Atmos. Chem. Phys., 14, 6941–6952, https://doi.org/10.5194/acp-14-6941-2014, 2014.

Novelli, A., Vereecken, L., Lelieveld, J., and Harder, H.: Direct observation of OH formation from stabilised Criegee intermediates, Phys. Chem. Chem. Phys., 16, 19941–19951, https://doi.org/10.1039/c4cp02719a, 2014.

Orlando, J. J. and Tyndall, G. S.: Laboratory studies of organic peroxy radical chemistry: an overview with emphasis on recent issues of atmospheric significance, Chem. Soc. Rev., 41, 6294–6317, https://doi.org/10.1039/C2CS35166H, 2012.

Orlando, J. J., Nozière, B., Tyndall, G. S., Orzechowska, G. E., Paulson, S. E., and Rudich, Y.: Product studies of the OH- and ozone-initiated oxidation of some monoterpenes, J. Geophys. Res.-Atmos., 105, 11561–11572, https://doi.org/10.1029/2000JD900005, 2000.

Paulot, F., Crounse, J. D., Kjaergaard, H. G., Kürten, A., St. Clair, J. M., Seinfeld, J. H., and Wennberg, P. O.: Unexpected Epoxide Formation in the Gas-Phase Photooxidation of Isoprene, Science, 325, 730–733, https://doi.org/10.1126/science.1172910, 2009.

Peeters, J. and Müller, J.-F.: HO$_x$ radical regeneration in isoprene oxidation via peroxy radical isomerisations. II: experimental evidence and global impact, Phys. Chem. Chem. Phys., 12, 14227–14235, https://doi.org/10.1039/C0CP00811G, 2010.

Peeters, J., Müller, J.-F., Stavrakou, T., and Nguyen, V. S.: Hydroxyl Radical Recycling in Isoprene Oxidation Driven by Hydrogen Bonding and Hydrogen Tunneling: The Upgraded LIM1 Mechanism, J. Phys. Chem. A, 118, 8625–8643, https://doi.org/10.1021/jp5033146, 2014.

Piccot, S. D., Watson, J. J., and Jones, J. W.: A global inventory of volatile organic compound emissions from anthropogenic sources, J. Geophys. Res.-Atmos., 97, 9897–9912, https://doi.org/10.1029/92JD00682, 1992.

Poppe, D., Brauers, T., Dorn, H.-P., Karl, M., Mentel, T., Schlosser, E., Tillmann, R., Wegener, R., and Wahner, A.: OH-initiated degradation of several hydrocarbons in the atmosphere simulation chamber SAPHIR, J. Atmos. Chem., 57, 203–214, https://doi.org/10.1007/s10874-007-9065-y, 2007.

Reissell, A., Harry, C., Aschmann, S. M., Atkinson, R., and Arey, J.: Formation of acetone from the OH radical- and O$_3$-initiated reactions of a series of monoterpenes, J. Geophys. Res.-Atmos., 104, 13869–13879, https://doi.org/10.1029/1999JD900198, 1999.

Ren, X., Olson, J. R., Crawford, J. H., Brune, W. H., Mao, J., Long, R. B., Chen, G., Avery, M. A., Sachse, G. W., Barrick, J. D., Diskin, G. S., Huey, L. G., Fried, A., Cohen, R. C., Heikes, B., Wennberg, P., Singh, H. B., Richard, D. R. B., and Shetter, E.: HOx Chemistry during INTEX-A 2004: Observation, Model Calculations and comparison with previous studies, J. Geophys. Res., 113, D05310, https://doi.org/10.1029/2007JD009166, 2008.

Ridley, B. A., Grahek, F. E., and Walega, J. G.: A Small High-Sensitivity, Medium-Response Ozone Detector Suitable for Measurements from Light Aircraft, J. Atmos. Ocean. Tech., 9, 142–148, https://doi.org/10.1175/1520-0426(1992)009<0142:ASHSMR>2.0.CO;2, 1992.

Rohrer, F. and Brüning, D.: Surface NO and NO$_2$ mixing ratios measured between 30° N and 30° S in the Atlantic region, J. Atmos. Chem., 15, 253–267, https://doi.org/10.1007/BF00115397, 1992.

Rohrer, F., Bohn, B., Brauers, T., Brüning, D., Johnen, F.-J., Wahner, A., and Kleffmann, J.: Characterisation of the photolytic HONO-source in the atmosphere simulation chamber SAPHIR, Atmos. Chem. Phys., 5, 2189–2201, https://doi.org/10.5194/acp-5-2189-2005, 2005.

Saathoff, H., Naumann, K.-H., Möhler, O., Jonsson, Å. M., Hallquist, M., Kiendler-Scharr, A., Mentel, Th. F., Tillmann, R., and Schurath, U.: Temperature dependence of yields of secondary organic aerosols from the ozonolysis of α-pinene and limonene, Atmos. Chem. Phys., 9, 1551–1577, https://doi.org/10.5194/acp-9-1551-2009, 2009.

Saunders, S. M., Jenkin, M. E., Derwent, R. G., and Pilling, M. J.: Protocol for the development of the Master Chemical Mechanism, MCM v3 (Part A): tropospheric degradation of non-aromatic volatile organic compounds, Atmos. Chem. Phys., 3, 161–180, https://doi.org/10.5194/acp-3-161-2003, 2003.

Schlosser, E., Bohn, B., Brauers, T., Dorn, H.-P., Fuchs, H., Häseler, R., Hofzumahaus, A., Holland, F., Rohrer, F., Rupp, L. O., Siese, M., Tillmann, R., and Wahner, A.: Intercomparison of Two Hydroxyl Radical Measurement Techniques at the Atmosphere Simulation Chamber SAPHIR, J. Atmos. Chem., 56, 187–205, https://doi.org/10.1007/s10874-006-9049-3, 2007.

Schlosser, E., Brauers, T., Dorn, H.-P., Fuchs, H., Häseler, R., Hofzumahaus, A., Holland, F., Wahner, A., Kanaya, Y., Kajii, Y., Miyamoto, K., Nishida, S., Watanabe, K., Yoshino, A., Kubistin, D., Martinez, M., Rudolf, M., Harder, H., Berresheim, H., Elste, T., Plass-Dülmer, C., Stange, G., and Schurath, U.: Technical Note: Formal blind intercomparison of OH measurements: results from the international campaign HOxComp, Atmos. Chem. Phys., 9, 7923–7948, https://doi.org/10.5194/acp-9-7923-2009, 2009.

Seinfeld, J. H. and Pandis, S. N.: Atmospheric Chemistry and Physics From Air Pollution to Climate Change, John Willey & Sons, Inc., 2 edn., 2006.

Sindelarova, K., Granier, C., Bouarar, I., Guenther, A., Tilmes, S., Stavrakou, T., Müller, J.-F., Kuhn, U., Stefani, P., and Knorr, W.: Global data set of biogenic VOC emissions calculated by the MEGAN model over the last 30 years, Atmos. Chem. Phys., 14, 9317–9341, https://doi.org/10.5194/acp-14-9317-2014, 2014.

Tan, D., Faloona, I., Simpas, J. B., Brune, W., Shepson, P. B., Couch, T. L., Sumner, A. L., Carroll, M. A., Thornberry, T., Apel, E., Riemer, D., and Stockwell, W.: HO$_x$ budgets in a deciduous forest: Results from the PROPHET summer 1998 campaign, J. Geophys. Res.-Atmos., 106, 24407–24427, https://doi.org/10.1029/2001jd900016, 2001.

Tan, Z., Fuchs, H., Lu, K., Hofzumahaus, A., Bohn, B., Broch, S., Dong, H., Gomm, S., Häseler, R., He, L., Holland, F., Li, X., Liu, Y., Lu, S., Rohrer, F., Shao, M., Wang, B., Wang, M., Wu, Y., Zeng, L., Zhang, Y., Wahner, A., and Zhang, Y.: Radical chemistry at a rural site (Wangdu) in the North China Plain: observation and model calculations of OH, HO$_2$ and RO$_2$ radicals, Atmos. Chem. Phys., 17, 663–690, https://doi.org/10.5194/acp-17-663-2017, 2017.

Taraborrelli, D., Lawrence, M. G., Crowley, J. N., Dillon, T. J., Gromov, S., Gross, C. B. M., Vereecken, L., and

Lelieveld, J.: Hydroxyl radical buffered by isoprene oxidation over tropical forests, Nat. Geosci., 5, 190–193, https://doi.org/10.1038/NGEO1405, 2012.

Vereecken, L. and Peeters, J.: A theoretical study of the OH-initiated gas-phase oxidation mechanism of β-pinene ($C^{10}H^{16}$) first generation products, Phys. Chem. Chem. Phys., 14, 3802–3815, https://doi.org/10.1039/C2CP23711C, 2012.

Wegener, R., Brauers, T., Koppmann, R., Rodríguez Bares, S., Rohrer, F., Tillmann, R., Wahner, A., Hansel, A., and Wisthaler, A.: Simulation chamber investigation of the reactions of ozone with short-chained alkenes, J. Geophys. Res.-Atmos., 112, D13301, https://doi.org/10.1029/2006jd007531, 2007.

Whalley, L. K., Edwards, P. M., Furneaux, K. L., Goddard, A., Ingham, T., Evans, M. J., Stone, D., Hopkins, J. R., Jones, C. E., Karunaharan, A., Lee, J. D., Lewis, A. C., Monks, P. S., Moller, S. J., and Heard, D. E.: Quantifying the magnitude of a missing hydroxyl radical source in a tropical rainforest, Atmos. Chem. Phys., 11, 7223–7233, https://doi.org/10.5194/acp-11-7223-2011, 2011.

Wiedinmyer, C., Guenther, A., Harley, P., Hewitt, N., Geron, C., Artaxo, P., Steinbrecher, R., and Rasmussen, R.: Global Organic Emissions from Vegetation, Springer Netherlands, vol. 18, 115–170, https://doi.org/10.1007/978-1-4020-2167-1_4, 2004.

Wisthaler, A., Jensen, N. R., Winterhalter, R., Lindinger, W., and Hjorth, J.: Measurements of acetone and other gas phase product yields from the OH-initiated oxidation of terpenes by proton-transfer-reaction mass spectrometry (PTR-MS), Atmos. Environ., 35, 6181–6191, https://doi.org/10.1016/s1352-2310(01)00385-5, 2001.

Wolfe, G. M., Crounse, J. D., Parrish, J. D., St. Clair, J. M., Beaver, M. R., Paulot, F., Yoon, T. P., Wennberg, P. O., and Keutsch, F. N.: Photolysis, OH reactivity and ozone reactivity of a proxy for isoprene-derived hydroperoxyenals (HPALDs), Phys. Chem. Chem. Phys., 14, 7276–7286, https://doi.org/10.1039/C2CP40388A, 2012.

Wolfe, G. M., Cantrell, C., Kim, S., Mauldin III, R. L., Karl, T., Harley, P., Turnipseed, A., Zheng, W., Flocke, F., Apel, E. C., Hornbrook, R. S., Hall, S. R., Ullmann, K., Henry, S. B., DiGangi, J. P., Boyle, E. S., Kaser, L., Schnitzhofer, R., Hansel, A., Graus, M., Nakashima, Y., Kajii, Y., Guenther, A., and Keutsch, F. N.: Missing peroxy radical sources within a summertime ponderosa pine forest, Atmos. Chem. Phys., 14, 4715–4732, https://doi.org/10.5194/acp-14-4715-2014, 2014.

Zhao, D. F., Kaminski, M., Schlag, P., Fuchs, H., Acir, I.-H., Bohn, B., Häseler, R., Kiendler-Scharr, A., Rohrer, F., Tillmann, R., Wang, M. J., Wegener, R., Wildt, J., Wahner, A., and Mentel, Th. F.: Secondary organic aerosol formation from hydroxyl radical oxidation and ozonolysis of monoterpenes, Atmos. Chem. Phys., 15, 991–1012, https://doi.org/10.5194/acp-15-991-2015, 2015.